Bianchi, M. E. (2007). DAMPs, PAMPs and alarmins: All we need to know about danger. *J. Leukoc. Biol.* **81,** 1–5.

Bryant, C., and Fitzgerald, K. A. (2009). Molecular mechanisms involved in inflammasome activation. *Trends Cell Biol.* **19,** 455–464.

Chaudhry, A. S., Urban, T. J., Lamba, J. K., Birnbaum, A. K., Remmel, R. P., Subramanian, M., Strom, S., You, J. H., Kasperaviciute, D., Catarino, C. B., *et al.* (2010). CYP2C9*1B promoter polymorphisms, in linkage with CYP2C19*2, affect phenytoin autoinduction of clearance and maintenance dose. *J. Pharmacol. Exp. Ther.* **332,** 599–611.

Cuttle, L., Munns, A. J., Hogg, N. A., Scott, J. R., Hooper, W. D., Dickinson, R. G., and Gillam, E. M. (2000). Phenytoin metabolism by human cytochrome P450: involvement of P450 3A and 2C forms in secondary metabolism and drug-protein adduct formation. *Drug Metab. Dispos.* **28,** 945–950.

Dhar, G. J., Pierach, C. A., Ahamed, P. N., and Howard, R. B. (1974). Diphenylhydantoin–induced hepatic necrosis. *Postgrad. Med.* **56,** 128–134.

Drew, R., and Miners, J. O. (1984). The effects of buthionine sulphoximine (BSO) on glutathione depletion and xenobiotic biotransformation. *Biochem. Pharmacol.* **33,** 2989–2994.

Fleishaker, J. C., Pearson, L. K., and Peters, G. R. (1995). Phenytoin causes a rapid increase in 6 beta-hydroxycortisol urinary excretion in humans–A putative measure of CYP3A induction. *J. Pharm. Sci.* **84,** 292–294.

Griffith, O. W., and Meister, A. (1979). Potent and specific inhibition of glutathione synthesis by buthionine sulfoximine (S-n-butyl homocysteine sulfoximine). *J. Biol. Chem.* **254,** 7558–7560.

Hagemeyer, C. E., Bürck, C., Schwab, R., Knoth, R., and Meyer, R. P. (2010). 7-Benzyloxyresorufin-O-dealkylase activity as a marker for measuring cytochrome P450 CYP3A induction in mouse liver. *Anal. Biochem.* **398,** 104–111.

Haruda, F. (1979). Phenytoin hypersensitivity: 38 cases. *Neurology* **29,** 1480–1485.

Higuchi, S., Yano, A., Takai, S., Tsuneyama, K., Fukami, T., Nakajima, M., and Yokoi, T. (2012). Metabolic activation and inflammation reactions involved in carbamazepine-induced liver injury. *Toxicol. Sci.* **130,** 4–16.

Kidd, P. (2003). Th1/Th2 balance: The hypothesis, its limitations, and implications for health and disease. *Altern. Med. Rev.* **8,** 223–246.

Kita, H., Mackay, I. R., Van De Water, J., and Gershwin, M. E. (2001). The lymphoid liver: Considerations on pathways to autoimmune injury. *Gastroenterology* **120,** 1485–1501.

Kobayashi, E., Kobayashi, M., Tsuneyama, K., Fukami, T., Nakajima, M., and Yokoi, T. (2009). Halothane-induced liver injury is mediated by interleukin-17 in mice. *Toxicol. Sci.* **111,** 302–310.

Kobayashi, M., Higuchi, S., Ide, M., Nishikawa, S., Fukami, T., Nakajima, M., and Yokoi, T. (2012). Th2 cytokine-mediated methimazole-induced acute liver injury in mice. *J. Appl. Toxicol.* **32,** 823–833.

Langrish, C. L., Chen, Y., Blumenschein, W. M., Mattson, J., Basham, B., Sedgwick, J. D., McClanahan, T., Kastelein, R. A., and Cua, D. J. (2005). IL-23 drives a pathogenic T cell population that induces autoimmune inflammation. *J. Exp. Med.* **201,** 233–240.

Latz, E. (2010). The inflammasomes: Mechanisms of activation and function. *Curr. Opin. Immunol.* **22,** 28–33.

Martinon, F., Mayor, A., and Tschopp, J. (2009). The inflammasomes: Guardians of the body. *Annu. Rev. Immunol.* **27,** 229–265.

Mullick, F. G., and Ishak, K. G. (1980). Hepatic injury associated with diphenylhydantoin therapy. A clinicopathologic study of 20 cases. *Am. J. Clin. Pathol.* **74,** 442–452.

Munns, A. J., De Voss, J. J., Hooper, W. D., Dickinson, R. G., and Gillam, E. M. (1997). Bioactivation of phenytoin by human cytochrome P450: Characterization of the mechanism and targets of covalent adduct formation. *Chem. Res. Toxicol.* **10,** 1049–1058.

Ong, M. M., Wang, A. S., Leow, K. Y., Khoo, Y. M., and Boelsterli, U. A. (2006). Nimesulide-induced hepatic mitochondrial injury in heterozygous Sod2(+/-) mice. *Free Radic. Biol. Med.* **40,** 420–429.

Oo, Y. H., and Adams, D. H. (2010). The role of chemokines in the recruitment of lymphocytes to the liver. *J. Autoimmun.* **34,** 45–54.

Roy, D., and Snodgrass, W. R. (1990). Covalent binding of phenytoin to protein and modulation of phenytoin metabolism by thiols in A/J mouse liver microsomes. *J. Pharmacol. Exp. Ther.* **252,** 895–900.

Scaffidi, P., Misteli, T., and Bianchi, M. E. (2002). Release of chromatin protein HMGB1 by necrotic cells triggers inflammation. *Nature* **418,** 191–195.

Schroder, K., and Tschopp, J. (2010). The inflammasomes. *Cell* **140,** 821–832.

Schwabe, R. F., Seki, E., and Brenner, D. A. (2006). Toll-like receptor signaling in the liver. *Gastroenterology* **130,** 1886–1900.

Shaw, P. J., Ditewig, A. C., Waring, J. F., Liguori, M. J., Blomme, E. A., Ganey, P. E., and Roth, R. A. (2009). Coexposure of mice to trovafloxacin and lipopolysaccharide, a model of idiosyncratic hepatotoxicity, results in a unique gene expression profile and interferon gamma-dependent liver injury. *Toxicol. Sci.* **107,** 270–280.

Shimizu, S., Atsumi, R., Itokawa, K., Iwasaki, M., Aoki, T., Ono, C., Izumi, T., Sudo, K., and Okazaki, O. (2009). Metabolism-dependent hepatotoxicity of amodiaquine in glutathione-depleted mice. *Arch. Toxicol.* **83,** 701–707.

Shimizu, S., Atsumi, R., Nakazawa, T., Izumi, T., Sudo, K., Okazaki, O., and Saji, H. (2011). Ticlopidine-induced hepatotoxicity in a GSH-depleted rat model. *Arch. Toxicol.* **85,** 347–353.

Spielberg, S. P., Gordon, G. B., Blake, D. A., Goldstein, D. A., and Herlong, H. F. (1981). Predisposition to phenytoin hepatotoxicity assessed in vitro. *N. Engl. J. Med.* **305,** 722–727.

Steinman, L. (2007). A brief history of T(H)17, the first major revision in the T(H)1/T(H)2 hypothesis of T cell-mediated tissue damage. *Nat. Med.* **13,** 139–145.

Talpain, E., Armstrong, R. A., Coleman, R. A., and Vardey, C. J. (1995). Characterization of the PGE receptor subtype mediating inhibition of superoxide production in human neutrophils. *Br. J. Pharmacol.* **114,** 1459–1465.

Taylor, J. W., Stein, M. N., Murphy, M. J., and Mitros, F. A. (1984). Cholestatic liver dysfunction after long-term phenytoin therapy. *Arch. Neurol.* **41,** 500–501.

Tietze, F. (1969). Enzymic method for quantitative determination of nanogram amounts of total and oxidized glutathione: Applications to mammalian blood and other tissues. *Anal. Biochem.* **27,** 502–522.

Watanabe, T., Sagisaka, H., Arakawa, S., Shibaya, Y., Watanabe, M., Igarashi, I., Tanaka, K., Totsuka, S., Takasaki, W., and Manabe, S. (2003). A novel model of continuous depletion of glutathione in mice treated with L-buthionine (S,R)-sulfoximine. *J. Toxicol. Sci.* **28,** 455–469.

Winn, L. M., and Wells, P. G. (1995). Phenytoin-initiated DNA oxidation in murine embryo culture, and embryo protection by the antioxidative enzymes superoxide dismutase and catalase: Evidence for reactive oxygen species-mediated DNA oxidation in the molecular mechanism of phenytoin teratogenicity. *Mol. Pharmacol.* **48,** 112–120.

Winn, L. M., and Wells, P. G. (1999). Maternal administration of superoxide dismutase and catalase in phenytoin teratogenicity. *Free Radic. Biol. Med.* **26,** 266–274.

Yamazaki, H., Komatsu, T., Takemoto, K., Saeki, M., Minami, Y., Kawaguchi, Y., Shimada, N., Nakajima, M., and Yokoi, T. (2001). Decreases in phenytoin hydroxylation activities catalyzed by liver microsomal cytochrome P450 enzymes in phenytoin-treated rats. *Drug Metab. Dispos.* **29,** 427–434.

Zhou, R., Tardivel, A., Thorens, B., Choi, I., and Tschopp, J. (2010). Thioredoxin-interacting protein links oxidative stress to inflammasome activation. *Nat. Immunol.* **11,** 136–140.

Zimmerman, H. J. (1999). *Hepatotoxicity: The Adverse Effects of Drugs and Other Chemicals on the Liver.* Lippncott Williams & Wilkins, Philadelphia, PA.

Downloaded from http://toxsci.oxfordjournals.org/ at Nagoya University on November 27, 2013

1521-009X/42/1/1–8$25.00
DRUG METABOLISM AND DISPOSITION
Copyright © 2013 by The American Society for Pharmacology and Experimental Therapeutics
http://dx.doi.org/10.1124/dmd.113.054478
Drug Metab Dispos 42:1–8, January 2014

DMD
DRUG METABOLISM AND DISPOSITION

Evaluation and Mechanistic Analysis of the Cytotoxicity of the Acyl Glucuronide of Nonsteroidal Anti-Inflammatory Drugs

Taishi Miyashita, Kento Kimura, Tatsuki Fukami, Miki Nakajima, and Tsuyoshi Yokoi

Drug Metabolism and Toxicology, Faculty of Pharmaceutical Sciences, Kanazawa University, Kanazawa, Japan

Received August 23, 2013; accepted October 8, 2013

ABSTRACT

The chemical reactivity of acyl glucuronide (AG) has been thought to be associated with the toxic properties of drugs containing carboxylic acid moieties, but there has been no direct evidence showing that AG formation is related to the observed toxicity. In the present study, the cytotoxicity of AGs, especially that associated with the inflammatory response, was investigated. The changes in the mRNA and protein expression levels of interleukin 8 (IL-8) and monocyte chemoattractant protein (MCP)-1 induced by the treatment of human peripheral blood mononuclear cells (PBMCs) with diclofenac (Dic), probenecid (Pro), tolmetin (Tol), ibuprofen (Ibu), naproxen (Nap), and their AGs were investigated by real-time reverse transcription polymerase chain reaction, and the viabilities of CD3+, CD14+, and CD19+ cells were measured by flow cytometry. Treatment with Dic-AG, Pro-AG, and Tol-AG significantly increased the expression levels of IL-8 and MCP-1. In addition, Dic-AG, Pro-AG, and Tol-AG significantly decreased the viability of CD14+ cells. Of these three AGs, Dic-AG showed the most potent changes, followed by Tol-AG and Pro-AG. Treatment with Ibu-AG and Nap-AG affected neither the expression levels of IL-8 and MCP-1 nor the viability of CD14+ cells. None of the drugs affected the CD3+ and CD19+ cell populations. Dic-AG increased the phosphorylation of p38 mitogen-activated protein (MAP) kinase and c-Jun N-terminal kinase (JNK)1/2. The pretreatment of peripheral blood mononuclear cells (PBMCs) with SB203580 (p38 inhibitor) significantly suppressed the Dic-AG-induced expression of inflammatory factors and cytotoxicity of CD14+ cells. In conclusion, AGs induce inflammatory responses and cytotoxicity against CD14+ cells via the p38 MAPK pathway. These factors may be useful biomarkers for evaluating the toxicity of AGs.

Introduction

Acyl glucuronidation is one of the major metabolic routes of drugs that contain carboxylic acid moieties. Glucuronidation is one of the most important phase II metabolic pathways for endogenous and exogenous substrates and is generally considered a detoxification pathway. However, it is well known that acyl glucuronides (AGs) are unstable under physiologic conditions and consequently undergo hydrolysis or intramolecular rearrangement through the migration of the drug moiety from the 1-*O*-position to the 2-, 3-, and 4-positions on the glucuronic acid ring (Smith et al., 1990; Benet et al., 1993; Bailey and Dickinson, 2003). AGs covalently modify endogenous proteins due to their electrophilic capacity to cause substitution reactions with the nucleophilic groups located on proteins or other macromolecules, and this effect can ultimately lead to adverse drug toxicities associated with carboxylic acid–containing drugs (Faed, 1984; Boelsterli, 2002). To date, both direct toxic effects and immune-mediated toxicity have been suggested as possible mechanisms of idiosyncratic liver injury. With direct toxicity, covalent protein binding via AG may disrupt the normal physiologic function of a "critical" protein or some critical regulatory pathway that lead to cellular necrosis (Pirmohamed et al., 1996). In addition, it has been reported that electrophilic AGs can covalently interact with nucleic acids. Clofibrate AG and gemfibrozil AG can form DNA adducts that result in genotoxicity, and these adducts can be measured through a single-cell gel electrophoresis (comet) assay (Sallustio et al., 2006). Furthermore, probenecid and clofibric acid have been found to induce DNA damage in isolated hepatocytes and uridine diphosphate (UDP)-glucuronosyltransferase (UGT)-transfected human embryonic kidney (HEK)293 (HEK/UGT) cells via a glucuronidation-dependent pathway (Sallustio et al., 2006; Southwood et al., 2007). Thus, there is increasing evidence that the formation of drug-protein adducts is involved in idiosyncratic reactions. However, we previously reported that the AGs of naproxen, diclofenac, ketoprofen, and ibuprofen do not lead to cytotoxicity or genotoxicity in HEK/UGT cells and human hepatocytes (Koga et al., 2011). Therefore, it is necessary to elucidate the possibility of immune- and/or inflammation-mediated toxicity to clarify the toxicity of AG. The potentially fatal adverse drug reactions most often appear to be immunologically based. These include anaphylactic reactions and severe dermatological reactions, such as Stevens-Johnson syndrome and fatal epidermal necrolysis (Bailey and Dickinson, 2003). In fact, it has been reported that mycophenolic acid, which is the active metabolite of the immunosuppressant mycophenolate mofetil, is primarily metabolized by glucuronidation to form an AG, which was found to result in the induction of cytokine [tumor necrosis

This study was supported by Health and Labor Sciences Research Grants from the Ministry of Health, Labor, and Welfare of Japan (H23-BIO-G001).
dx.doi.org/10.1124/dmd.113.054478.

aspet

ABBREVIATIONS: 7AAD, 7-amino-actinomycin D; AG, acyl glucuronide; Dic, diclofenac; ERK, extracellular signal-regulated kinase; GAPDH, glyceraldehyde 3-phosphate dehydrogenase; HEK, human embryonic kidney; Ibu, ibuprofen; IDT, idiosyncratic drug toxicity; IL, interleukin; JNK, c-Jun N-terminal kinase; MAPK, mitogen-activated protein kinase; MCP, monocyte chemoattractant protein; Nap, naproxen; NSAID, nonsteroidal anti-inflammatory drugs; PBMCs, peripheral blood mononuclear cells; PI, propidium iodide; Pro, probenecid; RT-PCR, reverse-transcription polymerase chain reaction; TNF, tumor necrosis factor; Tol, tolmetin; UGT, UDP-glucuronosyltransferase.

factor alpha (TNFα) and interleukin (IL)-6)] formation in leukocytes in a cell-based study (Wieland et al., 2000). It could be envisaged that the induction of immune modulators can lead to immune- and/or inflammation-related adverse drug reactions.

Of the drugs containing carboxylic acid moieties, diclofenac (Dic), probenecid (Pro), tolmetin (Tol), ibuprofen (Ibu), and naproxen (Nap), and their AGs were selected for the present study (Fig. 1). These drugs containing carboxylic acid are associated with some degree of hepatotoxicity, immune cytopenias, and hypersensitivity reactions in patients (Bailey and Dickinson, 2003) and have been categorized as potentially idiosyncratic drug toxicity (IDT) drugs in RxList (the Internet drug index system) or in Japanese drug labeling. Therefore, it is suggested that the AGs of these drugs may be related to their toxicity. The purpose of this study was to investigate whether AGs induce the observed cytotoxicity, particularly through inflammatory responses, and to clarify the involvement of cell signaling in the cytotoxicity.

Materials and Methods

Diclofenac sodium salt (Dic) and (S)-(+)-6-methoxy-α-methyl-2-naphthaleneacetic acid (Nap) were purchased from Sigma-Aldrich (St. Louis, MO). Ibuprofen (Ibu) and probenecid (Pro) were purchased from Wako Pure Chemicals (Osaka, Japan). Tolmetin (Tol) was purchased from LKT Laboratories (St. Paul, MN). 4′-Hydroxy diclofenac (4′-OH Dic), 5-hydroxy diclofenac (5-OH Dic), diclofenac acyl-β-D-glucuronide (Dic-AG), and other AGs were obtained from Toronto Research Chemicals (North York, ON, Canada). Propidium iodide (PI) and 7-amino-actinomycin D (7-AAD) were purchased from BD Pharmingen (San Diego, CA). Monoclonal antibodies against extracellular signal-regulated kinase (ERK)1/2 and c-Jun N-terminal kinase (JNK)1/2 and the polyclonal antibody against p38 mitogen-activated protein kinase (MAPK) were purchased from Cell Signaling Technology (Beverly, MA). Monoclonal antibodies against anti-Thr202/Tyr204 phosphorylated ERK1/2, anti-Thr180/Tyr182 phosphorylated p38 MAPK, and anti-Thr183/Tyr185 phosphorylated JNK1/2 were also obtained from Cell Signaling Technology. IRDye680-labeled goat anti-rabbit or anti-mouse secondary antibody and Odyssey Blocking Buffer were purchased from Li-COR Biosciences (Lincoln, NE). All of the primers were commercially synthesized at Hokkaido System Sciences (Sapporo, Japan). All other reagents were of the highest commercially available grade.

Cell Culture. The human monocytic leukemia cell line THP-1 was obtained from Riken Gene Bank (Tsukuba, Japan). Human peripheral blood mononuclear cells (PBMCs; lot no. 48) and CTL-Test medium for the culture of PBMCs were obtained from Cellular Technology (Shaker Heights, OH). Human "total liver cells" (primary culture of the mixed population of all native human liver cells) were obtained from SciKon Innovation (Chapel Hill, NC). The THP-1 cells were cultured in RPMI 1640 medium (Nissui Pharmaceutical, Tokyo, Japan) supplemented with 10% fetal bovine serum (FBS; Invitrogen, Carlsbad, CA). The total liver cells were cultured in Hepatocyte Basal Medium (HBM) supplemented with Hepatocyte Culture Media (HCM) SingleQuots (Lonza, Basel, Switzerland), and these cells were maintained at 37°C under an atmosphere of 5% CO_2.

The THP-1 cells, PBMCs, and total liver cells were seeded at densities of 1×10^6, 3×10^6, and 7.5×10^5 cells/well, respectively, in a 24-well plate with medium containing the indicated concentration of the selected carboxylic acid–containing drugs and their AG and then incubated at 37°C. The final concentration of methanol in the culture medium was 0.1% in all of the experiments. The supernatants were separated from the cell cultures by centrifugation and stored at –80°C until assayed.

Real-Time Reverse Transcription Polymerase Chain Reaction. The total RNA was extracted from each cell using RNAiso (Takara Bio, Shiga, Japan) according to the protocol supplied by manufacturer. The reverse transcription was performed with ReverTra Ace (Toyobo, Tokyo, Japan) according to the manufacturer's protocol. For quantitative analysis of the mRNA levels of inflammatory cytokines, real-time reverse transcription polymerase chain reaction (RT-PCR) was performed using an MX3000P real-time PCR system (Stratagene, La Jolla, CA). The primers used in this study were human IL-8 (forward: 5′-CAGCCTTCCTG ATTTCTCTGCAG-3′, reverse: 5′-AGACAGAGCTCTCTTCCATCAG-3′) and human monocyte chemoattractant protein (MCP)-1 (forward 5′-ACCGAGAGGCTGAGACTAAC-3′, reverse: 5′-CAGGTGACTGGGGCATTGAT-3′). A 1-μl volume of the reverse-transcribed mixture was added to a PCR mixture containing 10 pmol of each primer and 10 μl of SYBR Premix ExTaq solution; the final volume of the reaction mixture was 20 μl. After an initial denaturation at 95°C for 30 seconds, the amplification was performed through 45 cycles of either denaturation at 94°C for 20 seconds and annealing and extension at 64°C for 20 seconds or denaturation at 94°C for 5 seconds, annealing at 64°C for 10 seconds, and extension at 74°C for 20 seconds. To normalize the RNA loading and PCR variations, the signals of the targets were normalized to the signals of human glyceraldehyde 3-phosphate dehydrogenase (GAPDH) mRNA (forward: 5′-CCATGAGAAGTATGACAACAGCC-3′, reverse: 5′-TGGGTGGCAGTGATGGCATGGA-3′).

Enzyme-Linked Immunosorbent Assay. The levels of the inflammatory chemokines IL-8 and MCP-1 in the cell supernatants were measured using the Human IL-8 ELISA Ready-SET-GO! and Human CCL2 (MCP-1) ELISA Ready-SET-GO! kits (eBioscience, San Diego, CA), respectively, according to the manufacturer's instructions.

Immunoblot Analysis. SDS-polyacrylamide gel electrophoresis and immunoblot analysis were performed. The cell homogenates (30 μg) were separated on 10% polyacrylamide gels and electrotransferred onto polyvinylidene difluoride membranes (Immobilon-P; Millipore Corporation, Billerica, MA). The membranes were probed with the monoclonal antibodies against anti-Thr202/Tyr204–phosphorylated ERK1/2, anti-Thr180/Tyr182–phosphorylated p38 MAPK, and anti-Thr183/Tyr185–phosphorylated JNK1/2 and

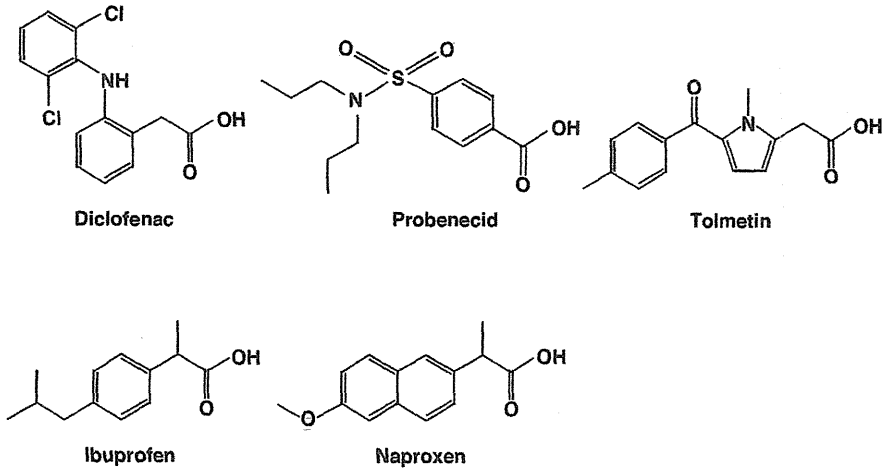

Fig. 1. Chemical structures of the NSAIDs investigated in this study: diclofenac, probenecid, tolmetin, ibuprofen, and naproxen.

incubated with IRDye680-labeled goat anti-rabbit or anti-mouse IgG secondary antibody diluted with phosphate-buffered saline with Tween-20. An Odyssey Infrared Imaging system (Li-COR Biosciences, Lincoln, NE) was used for the detection. The relative expression levels were quantified using the ImageQuant TL Image Analysis software (GE Healthcare, Little Chalfont, Buckinghamshire, UK).

Flow Cytometry Analysis. The PBMCs were washed with phosphate-buffered saline containing 0.1% bovine serum albumin. The cells were transferred to a 96-well plate and maintained on ice throughout the procedure until their analysis by flow cytometry. The PBMCs were stained using the following monoclonal antibodies: anti-human CD3-Pacific Blue (clone UCHT1; Invitrogen, Carlsbad, CA), anti-human CD14-PE (clone TüK4; Invitrogen) anti-human CD19-PE-Cy7 (clone SJ25-C1; Invitrogen). The monoclonal antibodies were diluted 1:10 in phosphate-buffered saline/0.1% bovine serum albumin, and the PBMC were incubated with these antibodies for 30 minutes in the dark. The PBMCs were washed and subsequently incubated with PI (0.625 μg/ml) or 7-AAD (0.25 μg/ml), and the cell viability was measured using an Attune Acoustic Focusing Cytometer (Applied Biosystems, Foster, CA).

Statistical Analyses. The data are presented as the means ± S.D. The comparison of the multiple groups was performed using analysis of variance (ANOVA) followed by the Dunnett or Tukey test. Differences with a P value of less than 0.05 were considered statistically significant.

Results

Effects of Dic-AG on mRNA Expression Levels of IL-8 and MCP-1 in THP-1 Cells, PBMCs, and Total Liver Cells. To investigate whether Dic-AG affects the expression levels of IL-8 and MCP-1 in THP-1 cells, PBMC, and total liver cells, the cells were treated with 100 μM Dic or Dic-AG for 24 hours, and the increase in the IL-8 and MCP-1 mRNA levels was measured. In THP-1 cells and PBMCs, the expression levels of IL-8 and MCP-1 were significantly increased by treatment with Dic-AG but not with vehicle (Ctl) or Dic (Fig. 2, A and B). The changes in the expression levels of these cytokines were higher in PBMCs compared with THP-1 cells: IL-8 (8.3-fold versus 1.7-fold) and MCP-1 (8.5-fold versus 4.7-fold). The total liver cells showed no response to Dic-AG (Fig. 2C). It was suggested that Dic-AG induced immune responses, although the changes in the expression levels of IL-8 and MCP-1 by Dic-AG were different in different cell types. PBMCs were used for the subsequent analyses because these cells demonstrated the highest sensitivity to AGs.

Dose- and Time-Dependent Effects of Dic-AG on IL-8 and MCP-1 mRNA Expression in and Protein Release from Human PBMCs. To investigate whether a low concentration of Dic-AG can affect the expression levels of inflammatory factors in PBMCs, these cells were treated with Dic, Dic-AG (0, 50, or 100 μM), or vehicle (1% methanol, Ctl) for 24 hours. As shown in Fig. 3A, Dic-AG increased the mRNA expression levels of IL-8 and MCP-1 in a dose-dependent manner. The time-dependent changes in the levels of IL-8 and MCP-1 mRNA in PBMCs after treatment with Dic-AG were investigated. Treatment with Dic-AG significantly increased the mRNA expression levels and the release of IL-8 and MCP-1 12 and 24 hours after treatment compared with those observed after treatment with Dic and vehicle (Fig. 3B). The time-dependent changes in the IL-8 and MCP-1 mRNA levels were reflected at the protein level (Fig. 3C); thus, the subsequent experiments mainly analyzed the changes in mRNA expression.

Effects of Dic-AG on Cell Populations of Human PBMCs. The effect of Dic-AG on the major cell populations of PBMCs (monocytes, T-lymphocytes, and B-lymphocytes) was investigated by flow cytometric analysis. The PBMCs were stained with fluorescent monoclonal antibodies against CD3 (T-lymphocyte), CD14 (monocyte), and CD19 (B-lymphocyte) and labeled with 7AAD or PI to detect the dead

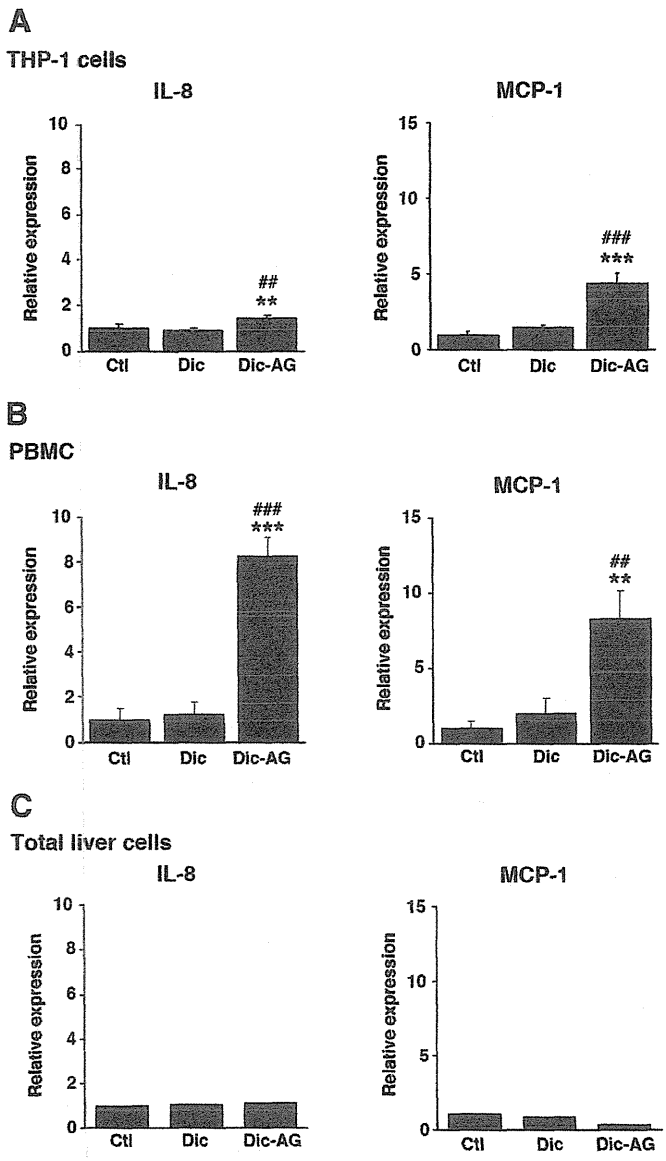

Fig. 2. Effects of Dic-AG on the expression levels of IL-8 and MCP-1 mRNA in THP-1 cells (A), human PBMCs (B), and total liver cells (C). The cells was treated with Dic, Dic-AG (100 μM), or vehicle (1% methanol, Ctl) for 24 hours. The IL-8 and MCP-1 mRNA levels were measured by real-time RT-PCR and normalized with GAPDH. The data represent the means ± S.D. (n = 4) or the mean (n = 2). $^{**}P < 0.01$ and $^{***}P < 0.001$ compared with Ctl. $^{\#\#}P < 0.01$ and $^{\#\#\#}P < 0.001$ compared with Dic.

cells. Treatment with Dic-AG markedly decreased the subset of $CD14^+$ cells of the total cells in a dose- and time-dependent manner (Fig. 4). This effect was not observed with Dic treatment. In addition, Dic-AG showed no inhibitory effect on either the $CD3^+$ cell population or the $CD19^+$ cell population (Fig. 4). These results suggest that Dic-AG specifically affects the viability of $CD14^+$ cells.

Effects of Various AGs on the mRNA Expression of IL-8 and MCP-1 in PBMCs and Their Cytotoxicity on $CD14^+$ Cells. To investigate whether various nonsteroidal anti-inflammatory drug (NSAID) AGs increase the expression levels of IL-8 and MCP-1 and decrease the subset of the $CD14^+$ cell population, PBMCs were treated with 100 μM NSAID or its AG for 24 hours; the mRNA levels of IL-8 and MCP-1 were then measured by real-time RT-PCR, and the cell viabilities of $CD3^+$, $CD14^+$, and $CD19^+$ cells were measured by

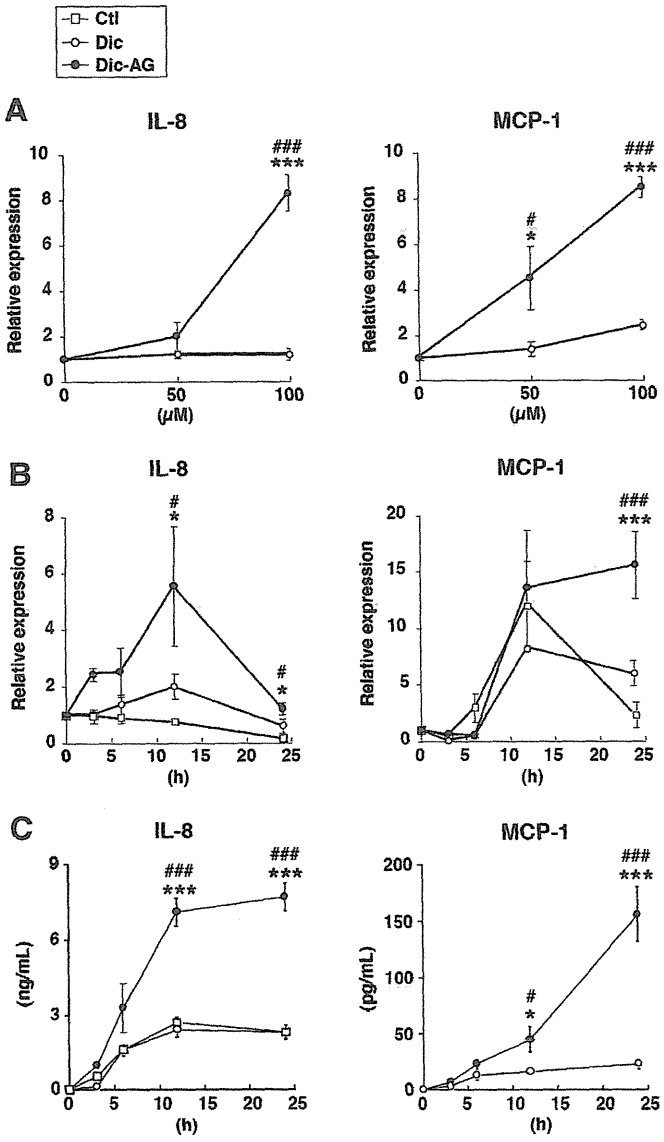

Fig. 3. Dose- and time-dependent effects of Dic-AG on the IL-8 and MCP-1 mRNA expression levels and protein release in human PBMCs. PBMCs were treated with Dic, Dic-AG (0, 50, or 100 μM), or vehicle (1% methanol, Ctl) for 24 hours (A) or with Dic or Dic-AG (100 μM) for 0, 3, 6, 12, and 24 hours (B). The IL-8 and MCP-1 mRNA levels were measured by real-time RT-PCR and normalized with GAPDH. The release of IL-8 and MCP-1 protein into the supernatant was measured by enzyme-linked immunosorbent assay (ELISA) (C). The data represent the means ± S.D. (n = 4). $^{*}P < 0.05$ and $^{***}P < 0.001$ compared with Ctl. $^{\#}P < 0.05$ and $^{\#\#\#}P < 0.001$ compared with Dic.

flow cytometry. As shown in Fig. 5, treatment with Pro-AG, Tol-AG, and Dic-AG significantly increased the expression levels of MCP-1 and IL-8. Furthermore, Pro-AG and Tol-AG significantly decreased the viability of $CD14^+$ cells. Treatment with Ibu-AG and Nap-AG affected neither the expression levels of IL-8 and MCP-1 nor the viability of $CD14^+$ cells. None of the AGs showed an inhibitory effect on either the $CD3^+$ cell population of the $CD19^+$ cell population. These results suggest that the AGs induced inflammatory factors and cytotoxicity against $CD14^+$ cells. Because Dic-AG had a pronounced effect on the expression of inflammatory factors and the viability of $CD14^+$ cells, further studies were performed to analyze the effect of Dic-AG.

Effects of Dic and Its Metabolites on mRNA Expression of IL-8 and MCP-1 and Cell Populations in Human PBMCs. Dic is metabolized to Dic-AG by UGT2B7 and to 4′-hydroxy Dic (4′-OH Dic) and 5-hydroxy Dic (5-OH Dic) by CYP2C9 and CYP3A4, respectively, in humans. It has been reported that these hydroxides are potential protoxicants because they can be further oxidized to quinone imine (van Leeuwen et al., 2011). To investigate whether Dic-AG and other metabolites might increase the expression levels of IL-8 and MCP-1 and decrease the $CD14^+$ cell population in PBMCs, PBMCs were treated with 100 μM Dic-AG, 4′-OH Dic, or 5-OH Dic for 24 hours, and the IL-8 and MCP-1 mRNA levels and the cell viability of $CD3^+$, $CD14^+$, and $CD19^+$ cells were then measured. As shown in Fig. 6, treatment with 4′-OH Dic and Dic-AG significantly increased the expression levels of IL-8 and MCP-1. Furthermore, Dic-AG and 4′-OH Dic significantly decreased the viability of $CD14^+$ cells. None of the compounds decreased the viability of $CD3^+$ and $CD19^+$ cells (data not shown). These results suggest that Dic-AG exhibits the highest cytotoxicity among these metabolites.

Effects of Dic-AG on the Activation of MAPK Signaling Pathways in Human PBMCs. The phosphorylation of MAPKs is a major component of many intracellular signaling pathways. To clarify the MAP kinase activation, the phosphorylation of ERK1/2 (44/42 kDa), p38 MAP kinase (43 kDa), and JNK1/2 (46/54 kDa) in cell lysates was assessed by immunoblot analysis. As shown in Fig. 7, Dic-AG treatment of 0.5 hours significantly increased the phosphorylation of p38 MAP kinase and JNK1/2 but not ERK1/2 in human PBMCs, which suggests that Dic-AG activates the p38 MAP kinase and JNK1/2 pathways in PBMCs. The phosphorylation of ERK1/2 was increased 12 hours after Dic-AG treatment (data not shown). To confirm the effects of MAP kinase inhibitors on the phosphorylation of ERK1/2, p38 MAP kinase, and JNK1/2, PBMC were pretreated for 1 hour with various concentrations of the MAPK/ERK kinase 1/2 inhibitor U0126, the p38 MAP kinase inhibitor SB203580, or the JNK1/2 inhibitor SP600125 before treatment with Dic-AG. The results show that the phosphorylations of p38 MAP kinase and JNK1/2 were significantly suppressed by pretreatment with their specific inhibitors (Fig. 5).

Effects of MAPK Inhibitors on Dic-AG-Induced Inflammatory Factors and Viability of $CD14^+$ Cells in Human PBMCs. To clarify which MAP kinase signaling pathway is mainly involved in the increase in expression levels of IL-8 and MCP-1 and in the decrease of $CD14^+$ cell population in PBMCs, the effects of MAP kinase inhibitors on the expression levels of IL-8 and MCP-1 and the viability of $CD14^+$ cells in PBMCs treated with Dic-AG were investigated. As shown in Fig. 8, the Dic-AG-induced increase in the level of IL-8 mRNA in PBMCs was significantly suppressed by pretreatment with SB203580 and SP600125, and the expression of MCP-1 was significantly suppressed by pretreatment with SB203580 and U0126. These findings suggest that the MAP kinase pathway plays an important role in the expression of IL-8 and MCP-1 in response to Dic-AG treatment. The decreased cell viability of $CD14^+$ cells by Dic-AG treatment was significantly restored by pretreatment with SB203580, which suggests that the p38 MAP kinase pathways are involved in the cytotoxicity of this drug in $CD14^+$ cells (Fig. 8B). These results indicate that the increase in the expression of inflammatory factors by Dic-AG treatment is partly related to the cytotoxic effects observed in $CD14^+$ cells.

Discussion

There is increasing evidence that the formation of drug-protein adducts is involved in idiosyncratic drug toxicities. However, little

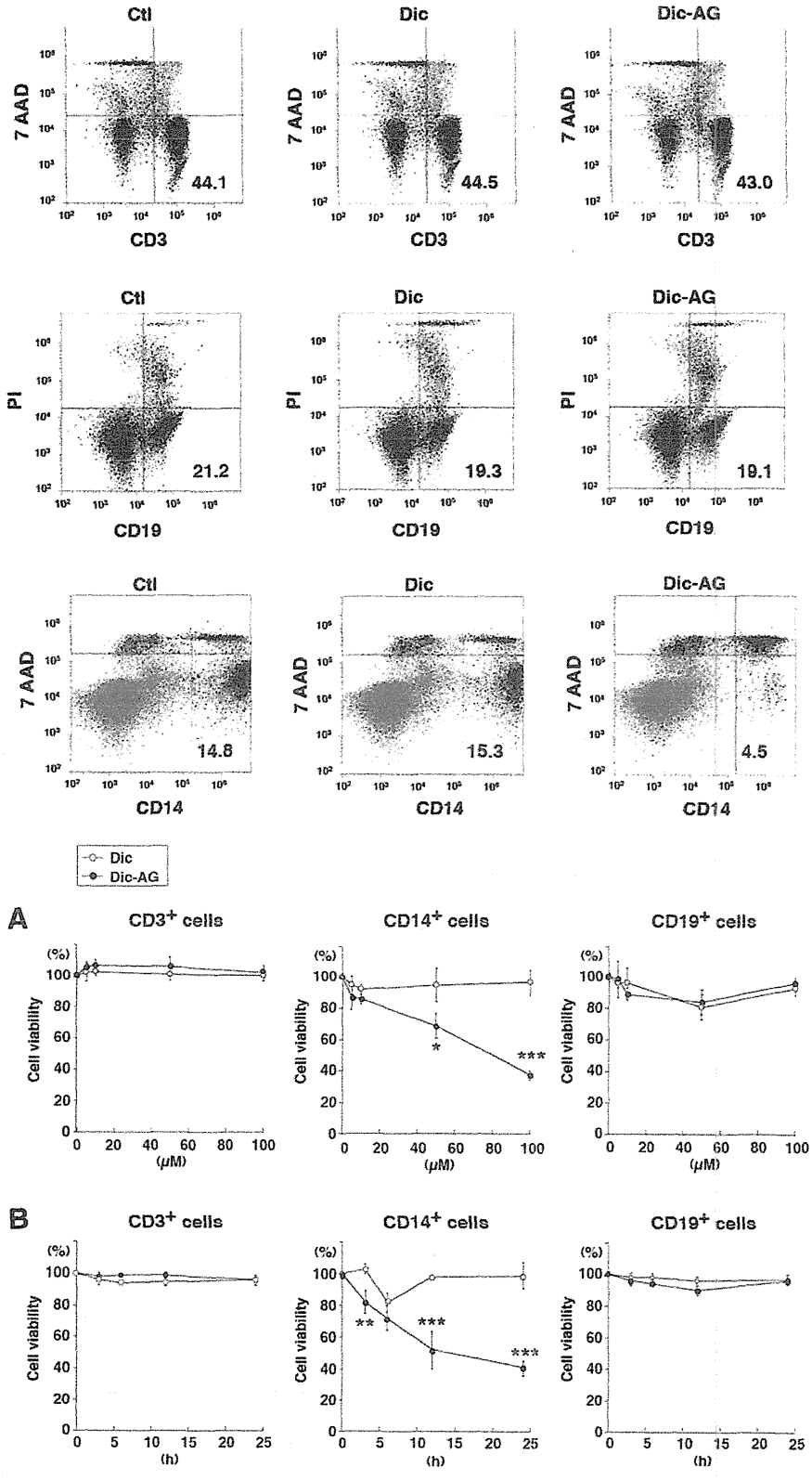

Fig. 4. Flow cytometry analysis of human PBMCs treated with Dic or Dic-AG. Flow cytometric bivariate frequency dot plots showing cell viability of CD3+, CD14, and CD19+ cells in PBMC treated with Dic, Dic-AG (100μM), or vehicle (1% methanol, Ctl) for 24 hours. Human PBMCs were treated with Dic, Dic-AG (0, 50, or 100 μM), or vehicle (1% methanol, Ctl) for 24 hours (A) or with Dic or Dic-AG (100 μM) for 0, 3, 6, 12, and 24 hours (B). The viability of $CD3^+$, $CD14^+$, and $CD19^+$ cells in PBMCs treated with Dic or Dic-AG was measured by PI or 7AAD assay, as described in *Materials and Methods*. The data represent the means ± S.D. ($n = 3$). $^*P < 0.05$, $^{**}P < 0.01$, and $^{***}P < 0.001$ compared with Dic.

direct evidence demonstrates a link between drug-protein adduct formation and adverse biologic consequences. It is well known that AGs are characterized by their electrophilic reactivity, and this reactivity is implicated in a wide range of adverse drug effects, including drug hypersensitivity reactions and cellular toxicity (Ritter, 2000). We previously revealed that the AGs of various NSAIDs, such as naproxen, diclofenac, ketoprofen, and ibuprofen, showed no direct cytotoxicity and genotoxicity in human hepatocytes and cells stably expressing human UGTs (Koga et al., 2011). Therefore, in this study, we investigated whether the AGs exert toxicity through inflammation-

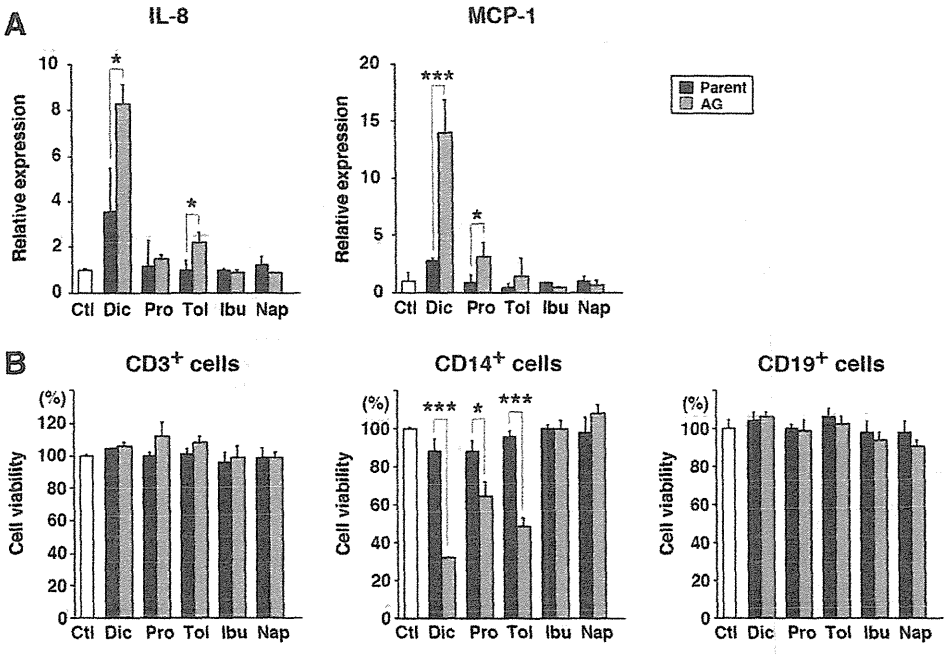

Fig. 5. Effects of NAIDs and their AGs on the mRNA expression levels of IL-8 and MCP-1 and their cytotoxicity to $CD3^+$, $CD14^+$, and $CD19^+$ cells in human PBMCs. Human PBMC were treated with Dic, Dic-AG, Pro, Pro-AG, Tol, Tol-AG, Ibu, Ibu-AG, Nap, Nap-AG (100 μM), or vehicle (1% methanol, Ctl) for 24 hours. The IL-8 and MCP-1 mRNA levels were measured by real-time RT-PCR and normalized with GAPDH (A). The cell viability of $CD14^+$ cells treated with Dic-AG was measured by 7AAD assay as described in *Materials and Methods* (B). The data represent the means ± S.D. (n = 4). $^*P < 0.05$ and $^{***}P < 0.001$ compared with the parent drugs.

related responses. Our previous research revealed that some drugs, such as albendazole, terbinafine, and amiodarone, stimulate THP-1 cells to release IL-8, which suggests the involvement of an inflammation-mediated pathway in drug-induced adverse reactions (Mizuno et al., 2010, 2011; Endo et al., 2012). Furthermore, it has been reported that cytokines and chemokines, such as MCP-1, are released by THP-1 cells and PBMCs after treatment with flavonoids or amyloid proteins (Song et al., 2009). Thus, the expression levels of IL-8 and MCP-1 as markers for predicting the activation of the inflammatory response induced by AGs were investigated in the present study.

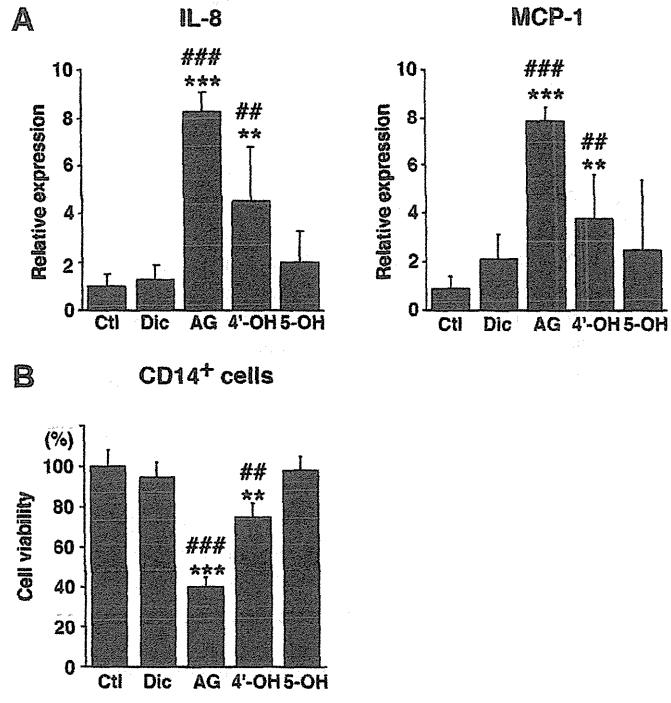

Fig. 6. Effects of Dic and its metabolites on the mRNA expression levels of IL-8 and MCP-1 in human PBMCs. Human PBMCs were treated with Dic, Dic-AG, 4'-OH Dic, 5-OH Dic (100 μM), or vehicle (1% methanol, Ctl) for 24 hours. The expression levels of IL-8 and MCP-1 mRNA were measured by real-time RT-PCR and normalized with GAPDH. The data represent the means ± S.D. (n = 4). $^{**}P < 0.01$ and $^{***}P < 0.001$ compared with Ctl. $^{\#\#}P < 0.01$ and $^{\#\#\#}P < 0.001$ compared with Dic.

First, the effects of Dic-AG treatment on three different types of cells, namely THP-1 cells, PBMCs, and total liver cells, were compared. We previously revealed that the NSAID AGs that were produced in the cells are efficiently released from the cells into the culture medium (Koga et al., 2011). Thus, the effect of AGs was evaluated by exposing the AGs to the outside of the cells, i.e., the culture medium. In a preliminary study, we found that Dic-AG treatment increases IL-8 production in human PBMCs (data not shown). Therefore, three cell types, namely THP-1 cells, PBMCs, and total liver cells, were exposed to Dic-AG treatment, and the treatment effects were compared. The expression levels of IL-8 and MCP-1 were significantly increased in THP-1 cells and PBMCs but not in total liver cells (Fig. 2). It has been reported that some inflammatory factors, such as IL-8, IL-10, and MCP-1, are released from mixed cell culture at a much higher level than that obtained from pure monocytes treated with proteins or chemicals (Feng et al., 2008). In addition, it has been reported that primary PBMCs are more sensitive to drugs and/or chemicals than tumor cells (Hougee et al., 2005). In this study, as suggested by previous reports, the inducibility of IL-8 and MCP-1 in PBMCs by Dic-AG treatment was much higher than that observed in THP-1 cells. We intended to evaluate the inflammatory responses in the liver by using total liver cells. However, the total liver cells are less sensitive to Dic-AG compared with THP-1 cells and PBMCs. The total liver cells were a primary culture of the mixed population of all native human liver cells, consisting mainly of hepatocytes and containing a low percentage of immune-related cells. From the present result, it was suggested that the total liver cells were not suitable for the sensitive in vitro cell-based assay.

Of the commercially available NSAID AGs, Dic-AG, Pro-AG, and Tol-AG induced the expression of IL-8 and MCP-1 and decreased the viability of $CD14^+$ cells. However, Ibu-AG and Nap-AG had no effect (Figs. 4 and 5). It was reported that the half-lives of Dic-AG, Pro-AG, and Tol-AG in potassium phosphate solution or human serum albumin

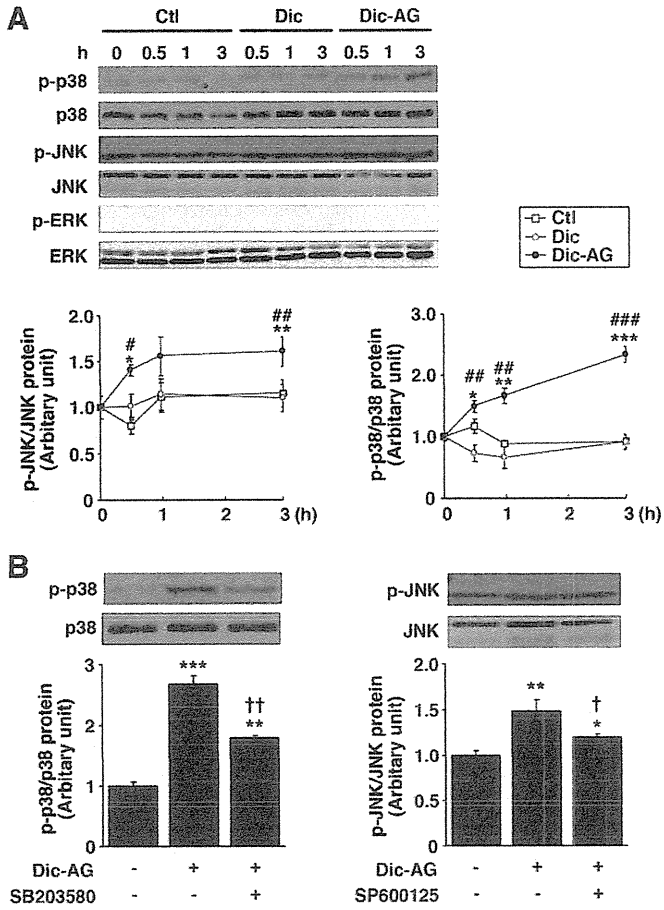

Fig. 7. Activation of MAP kinase signaling pathways in PBMCs treated with Dic-AG. Immunoblot analyses of the MAP kinase proteins in PBMCs were performed and quantified (A). Before treatment with 100 μM Dic-AG, the PBMCs were pretreated with the indicated concentrations of the MAP kinase inhibitors for 1 hour (B). U0126, SB203580, and SP600125 were used as specific inhibitors of MAPK/ERK kinase 1/2, p38 MAP kinase, and JNK1/2, respectively. After 0.5, 1, and 3 hours of incubation with Dic-AG, the cell lysates were subjected to immunoblot analyses using anti-Thr202/Tyr204 phosphorylated ERK1/2, anti-Thr180/Tyr182 phosphorylated p38 MAP kinase, and anti-Thr183/Tyr185 phosphorylated JNK1/2 antibodies. The data represent the means ± S.D. ($n = 3$). $^{*}P < 0.05$, $^{**}P < 0.01$, and $^{***}P < 0.001$ compared with Ctl. $^{\#}P < 0.05$, $^{\#\#}P < 0.01$, and $^{\#\#\#}P < 0.001$ compared with Dic. $^{\dagger}P < 0.05$ and $^{\dagger\dagger}P < 0.01$ compared with Dic-AG.

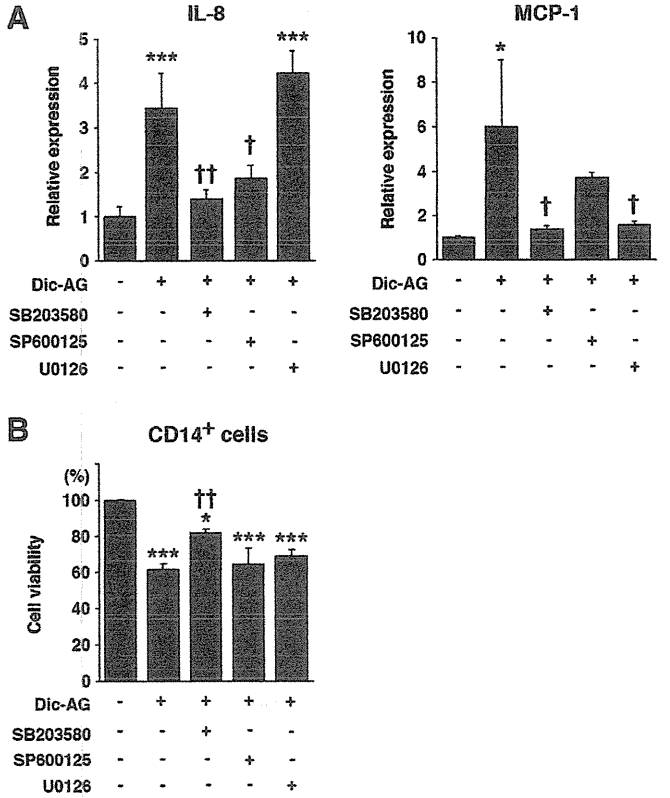

Fig. 8. Effects of MAP kinase inhibitors on Dic-AG-induced IL-8 and MCP-1 expression and cytotoxicity to $CD14^{+}$ cells in human PBMCs. Before treatment with 100 μM Dic-AG, the PBMCs were pretreated with the indicated concentrations of the MAP kinase inhibitors for 1 hour. After 24-hour incubation with Dic-AG, the expression levels of IL-8 and MCP-1 mRNA were measured by real-time RT-PCR, and the viability of $CD14^{+}$ cells treated with Dic-AG was measured by 7AAD assay as described in *Materials and Methods*. The data represent the means ± S.D. ($n = 3$). $^{*}P < 0.05$ and $^{***}P < 0.001$ compared with Ctl. $^{\dagger}P < 0.05$ and $^{\dagger\dagger}P < 0.01$ compared with Dic-AG.

are shorter than those of Ibu-AG and Nap-AG (Sawamura et al., 2010). Furthermore, a covalent binding study using a small peptide demonstrated that the degree of AG reactivity is affected by its chemical structure (Wang et al., 2004) (in descending order): acetic acid derivative > isopropionic acid derivative > benzoic acid derivative. It was hypothesized that the benzoic acid derivative exhibits the lowest reactivity due to the resonance stabilization provided by the aromatic moiety and that the isopropionic acid derivative displays a lower reactivity than that of the acetic acid derivative likely due to the higher steric hindrance capacity of the isopropyl group compared with the acetyl group (Wang et al., 2004). These reports suggest that the stability of AGs serve as a useful key predictor for their IDT risk. Thus, it was surmised that the observed increase in the levels of inflammatory factors and the cytotoxicity of $CD14^{+}$ cells by Dic-AG, Pro-AG, and Tol-AG may be related to the structural properties of the AGs.

Dic-AG is one of the most studied AGs due to its related toxicity. Dic-AG is excreted into bile and transported to the small intestine, where it can produce erosions and ulcers in a dose-dependent manner in rats (Seitz and Boelsterli, 1998). Dic is metabolized to Dic-AG by UGT2B7 and to 4′-hydroxy Dic (4′-OH Dic) and 5-hydroxy Dic (5-OH Dic) by CYP2C9 and CYP3A4, respectively. These hydroxides are further metabolized to form benzoquinone imine, which leads to the production of oxidative stress and covalent binding with endogenous proteins (Tang et al., 1999). Of these metabolites, 4′-OH Dic and Dic-AG increased the expression levels of IL-8 and MCP-1 (Fig. 6). The inducibility of these genes by Dic-AG was much higher than that obtained with 4′-OH Dic, which suggests that Dic-AG shows the highest cytotoxicity among these metabolites. It appeared important to evaluate the toxicity of not only the AG but also the quinone imines of Dic.

The activation of MAP kinases, such as ERK1/2, p38 MAP kinase, and JNK1/2, is important for the mediation of the monocyte and macrophage functions, including the activation of various transcription factors, the production of proinflammatory cytokines, and cell death (Payne et al., 1991; Defranco et al., 1998). In this study, Dic-AG activated the p38 MAP kinase and JNK1/2 pathways in PBMCs (Fig. 7A). The blocking of these MAP kinases by several MAP kinase inhibitors prevented the transcription and/or translation of IL-8 and MCP-1 from Lipopolysaccharide-stimulated monocytes and PBMCs (Guha and Mackman, 2001; Islam et al., 2006). To determine the involvement of MAP kinases in the Dic-AG-induced increase in the expression levels of IL-8 and MCP-1 and the cytotoxicity to $CD14^{+}$ cells, blocking studies were performed using specific inhibitors of

these MAP kinases, including U0126, SB203580, and SP600125 (English and Cobb, 2002). In this study, the p38 MAP kinase pathway was shown to be involved in the stimulation of the increase in the expression levels of IL-8 and MCP-1 in PBMCs (Fig. 8A) and the cytotoxicity to $CD14^+$ cells (Fig. 8B). In the future, it should be clarified whether $CD14^+$ monocytes are the main source of cell death–related inflammatory cytokines and chemokines (IL-8 and MCP-1) after treatment of PBMCs with a drug.

Notably, the circulating cell population of monocytes ($CD14^+$ cells) in the blood is continuously supplied in vivo from the bone marrow, and these cells migrate into the tissues (Hougee et al., 2005), which is an effect that cannot be reproduced under in vitro experimental conditions. It is reported that $CD14^+$ cells were specifically eliminated in PBMCs by apigenin and its structural analogs chrysin and luteolin. Thus, it is considered that the structures of the $CD14^+$ cell surface and of the drugs are important for the onset of toxicity. Therefore, the in vivo evaluation of the mechanism through which AGs exert their selective cytotoxicity to $CD14^+$ cells is required.

In conclusion, we demonstrated that AGs increase the inflammatory responses and cytotoxicity of CD14+ cells via the p38 MAP kinase pathway in human PBMCs. These factors could be useful biomarkers for evaluating the toxicity of AGs. This study provides new insights into the evaluation of the toxicity of AGs in drug development.

Authorship Contributions

Participated in research design: Miyashita, Fukami, Nakajima, Yokoi.
Conducted experiments: Miyashita, Kimura.
Contributed new reagents or analytic tools: Miyashita, Yokoi.
Performed data analysis: Miyashita.
Wrote or contributed to the writing of the manuscript: Miyashita, Yokoi.

References

Bailey MJ and Dickinson RG (2003) Acyl glucuronide reactivity in perspective: biological consequences. *Chem Biol Interact* **145**:117–137.

Benet LZ, Spahn-Langguth H, Iwakawa S, Volland C, Mizuma T, Mayer S, Mutschler E, and Lin ET (1993) Predictability of the covalent binding of acidic drugs in man. *Life Sci* **53**: PL141–PL146.

Boelsterli UA (2002) Xenobiotic acyl glucuronides and acyl CoA thioesters as protein-reactive metabolites with the potential to cause idiosyncratic drug reactions. *Curr Drug Metab* **3**: 439–450.

DeFranco AL, Crowley MT, Finn A, Hambleton J, and Weinstein SL (1998) The role of tyrosine kinases and map kinases in LPS-induced signaling. *Prog Clin Biol Res* **397**:119–136.

Endo S, Toyoda Y, Fukami T, Nakajima M, and Yokoi T (2012) Stimulation of human monocytic THP-1 cells by metabolic activation of hepatotoxic drugs. *Drug Metab Pharmacokinet* **27**: 621–630.

English JM and Cobb MH (2002) Pharmacological inhibitors of MAPK pathways. *Trends Pharmacol Sci* **23**:40–45.

Faed EM (1984) Properties of acyl glucuronides: implications for studies of the pharmacokinetics and metabolism of acidic drugs. *Drug Metab Rev* **15**:1213–1249.

Feng Y, Yang X, Liu Z, Liu Y, Su B, Ding Y, Qin L, Yang H, Zheng R, and Hu Z (2008) Continuous treatment with recombinant Mycobacterium tuberculosis CFP-10-ESAT-6 protein activated human monocyte while deactivated LPS-stimulated macrophage. *Biochem Biophys Res Commun* **365**:534–540.

Guha M and Mackman N (2001) LPS induction of gene expression in human monocytes. *Cell Signal* **13**:85–94.

Hougee S, Sanders A, Faber J, Graus YM, van den Berg WB, Garssen J, Smit HF, and Hoijer MA (2005) Decreased pro-inflammatory cytokine production by LPS-stimulated PBMC upon in vitro incubation with the flavonoids apigenin, luteolin or chrysin, due to selective elimination of monocytes/macrophages. *Biochem Pharmacol* **69**:241–248.

Islam Z, Gray JS, and Pestka JJ (2006) p38 Mitogen-activated protein kinase mediates IL-8 induction by the ribotoxin deoxynivalenol in human monocytes. *Toxicol Appl Pharmacol* **213**:235–244.

Koga T, Fujiwara R, Nakajima M, and Yokoi T (2011) Toxicological evaluation of acyl glucuronides of nonsteroidal anti-inflammatory drugs using human embryonic kidney 293 cells stably expressing human UDP-glucuronosyltransferase and human hepatocytes. *Drug Metab Dispos* **39**:54–60.

Mizuno K, Fukami T, Toyoda Y, Nakajima M, and Yokoi T (2010) Terbinafine stimulates the pro-inflammatory responses in human monocytic THP-1 cells through an ERK signaling pathway. *Life Sci* **87**:537–544.

Mizuno K, Toyoda Y, Fukami T, Nakajima M, and Yokoi T (2011) Stimulation of pro-inflammatory responses by mebendazole in human monocytic THP-1 cells through an ERK signaling pathway. *Arch Toxicol* **85**:199–207.

Payne DM, Rossomando AJ, Martino P, Erickson AK, Her JH, Shabanowitz J, Hunt DF, Weber MJ, and Sturgill TW (1991) Identification of the regulatory phosphorylation sites in pp42/mitogen-activated protein kinase (MAP kinase). *EMBO J* **10**:885–892.

Pirmohamed M, Madden S, and Park BK (1996) Idiosyncratic drug reactions. Metabolic bioactivation as a pathogenic mechanism. *Clin Pharmacokinet* **31**:215–230.

Ritter JK (2000) Roles of glucuronidation and UDP-glucuronosyltransferases in xenobiotic bioactivation reactions. *Chem Biol Interact* **129**:171–193.

Sallustio BC, Degraaf YC, Weekley JS, and Burcham PC (2006) Bioactivation of carboxylic acid compounds by UDP-Glucuronosyltransferases to DNA-damaging intermediates: role of glycoxidation and oxidative stress in genotoxicity. *Chem Res Toxicol* **19**:683–691.

Sawamura R, Okudaira N, Watanabe K, Murai T, Kobayashi Y, Tachibana M, Ohnuki T, Masuda K, Honma H, and Kurihara A, et al. (2010) Predictability of idiosyncratic drug toxicity risk for carboxylic acid-containing drugs based on the chemical stability of acyl glucuronide. *Drug Metab Dispos* **38**:1857–1864.

Seitz S and Boelsterli UA (1998) Diclofenac acyl glucuronide, a major biliary metabolite, is directly involved in small intestinal injury in rats. *Gastroenterology* **115**:1476–1482.

Smith PC, Benet LZ, and McDonagh AF (1990) Covalent binding of zomepirac glucuronide to proteins: evidence for a Schiff base mechanism. *Drug Metab Dispos* **18**:639–644.

Song C, Hsu K, Yamen E, Yan W, Fock J, Witting PK, Geczy CL, and Freedman SB (2009) Serum amyloid A induction of cytokines in monocytes/macrophages and lymphocytes. *Atherosclerosis* **207**:374–383.

Southwood HT, DeGraaf YC, Mackenzie PI, Miners JO, Burcham PC, and Sallustio BC (2007) Carboxylic acid drug-induced DNA nicking in HEK293 cells expressing human UDP-glucuronosyltransferases: role of acyl glucuronide metabolites and glycation pathways. *Chem Res Toxicol* **20**:1520–1527.

Tang W, Stearns RA, Bandiera SM, Zhang Y, Raab C, Braun MP, Dean DC, Pang J, Leung KH, and Doss GA, et al. (1999) Studies on cytochrome P-450-mediated bioactivation of diclofenac in rats and in human hepatocytes: identification of glutathione conjugated metabolites. *Drug Metab Dispos* **27**:365–372.

van Leeuwen JS, Vredenburg G, Dragovic S, Tjong TF, Vos JC, and Vermeulen NP (2011) Metabolism related toxicity of diclofenac in yeast as model system. *Toxicol Lett* **200**:162–168.

Wang J, Davis M, Li F, Azam F, Scatina J, and Talaat R (2004) A novel approach for predicting acyl glucuronide reactivity via Schiff base formation: development of rapidly formed peptide adducts for LC/MS/MS measurements. *Chem Res Toxicol* **17**:1206–1216.

Wieland E, Shipkova M, Schellhaas U, Schütz E, Niedmann PD, Armstrong VW, and Oellerich M (2000) Induction of cytokine release by the acyl glucuronide of mycophenolic acid: a link to side effects? *Clin Biochem* **33**:107–113.

Address correspondence to: Tsuyoshi Yokoi, Department of Drug Safety Sciences, Nagoya University Graduate School of Medicine, 65 Tsurumai-cho, Showa-ku, Nagoya,466-8550, Japan. E-mail: tyokoi@med.nagoya-u.ac.jp

Toxicology Letters 224 (2014) 215–224

Contents lists available at ScienceDirect

Toxicology Letters

journal homepage: www.elsevier.com/locate/toxlet

Involvement of oxidative stress and immune- and inflammation-related factors in azathioprine-induced liver injury

Kentaro Matsuo[a], Eita Sasaki[a], Satonori Higuchi[a], Shohei Takai[a], Koichi Tsuneyama[b], Tatsuki Fukami[a], Miki Nakajima[a], Tsuyoshi Yokoi[a,*,1]

[a] Drug Metabolism and Toxicology, Faculty of Pharmaceutical Sciences, Kanazawa University, Kakuma-machi, Kanazawa 920-1192, Japan
[b] Department of Diagnostic Pathology, Graduate School of Medicine and Pharmaceutical Science for Research, University of Toyama, Sugitani, 930-0194 Toyama, Japan

HIGHLIGHTS

- We developed a mouse model of AZA-induced liver injury.
- The mechanism of AZA-induced liver injury was investigated.
- Oxidative stress is involved in AZA-induced liver injury.
- Inflammatory response contributes in the exacerbation phase of liver injury.
- Activation of the innate immune system contributes to the exacerbation phase.

ARTICLE INFO

Article history:
Received 26 August 2013
Received in revised form 23 October 2013
Accepted 23 October 2013
Available online 30 October 2013

Keywords:
Azathioprine
Oxidative stress
Inflammation
Liver injury
Model mouse

ABSTRACT

Drug-induced liver injury (DILI) is a growing concern in the fields of drug development and clinical drug therapy because numerous drugs have been linked to hepatotoxicity. However, it is difficult to predict DILI in humans due to the lack of experimental animal models. Although azathioprine (AZA), which is a widely used immunosuppressive drug, is generally well tolerated, a small number of patients prescribed AZA develop severe hepatitis. However, the mechanism underlying this process has not yet been elucidated. In this study, we developed a mouse model of AZA-induced liver injury and investigated the mechanisms responsible for the hepatotoxicity of AZA. Female BALB/c mice were orally administered AZA. After AZA administration, the plasma levels of alanine aminotransferase and aspartate aminotransferase were increased, and liver damage was confirmed through a histological evaluation. In addition, the hepatic glutathione levels and superoxide dismutase activity were significantly decreased. The plasma levels of reactive oxygen species were significantly increased during the early phase of AZA-induced liver injury, and the hepatic mRNA levels of immune- and inflammation-related factors were also significantly changed. In conclusion, oxidative stress and the subsequently activated immune- and inflammation-related factors are involved in AZA-induced liver injury.

© 2013 Published by Elsevier Ireland Ltd.

1. Introduction

Drug-induced liver injury (DILI) is the most frequent reason for the withdrawal of a drug from the market and the cessation of new drug development by pharmaceutical companies. Due to their association with significant patient morbidity and mortality, several drugs, including bromfenac, ebrotidine, and troglitazone, have been removed from the pharmaceutical market (Holt and Ju, 2006). In most cases, the mechanisms of hepatotoxicity are unknown, and predictive experimental animal models are lacking.

Azathioprine (AZA) is an immunosuppressive drug that is often used to treat inflammatory bowel disease and autoimmune conditions, such as rheumatoid arthritis, and is often used after transplantation to avoid organ rejection (Dejaco et al., 2003; Maltzman and Koretzky, 2003; Dubinsky, 2004). However, its therapeutic potential is limited by its high incidence (15–28%) of adverse reactions, such as hepatotoxicity, bone marrow suppression, and gastrointestinal symptoms (Marinaki et al., 2004; Takatsu et al., 2009). In a prospective cohort study, the hepatotoxicity of AZA was recognized in approximately 2% of rheumatoid arthritis and psoriatic arthritis patients (Aithal, 2011). The hepatotoxicity of AZA was demonstrated *in vivo* in rats, which exhibited a less than

* Corresponding author. Tel.: +81 76 234 4407; fax: +81 76 234 4407.
E-mail addresses: tyokoi@p.kanazawa-u.ac.jp, tyokoi@kenroku.kanazawa-u.ac.jp (T. Yokoi).
[1] Present address: Department of Drug Safety Sciences Nagoya University Graduate School of Medicine 65 Tsurumai-cho, Showa-ku, Nagoya, 466-8550, Japan.

0378-4274/$ – see front matter © 2013 Published by Elsevier Ireland Ltd.
http://dx.doi.org/10.1016/j.toxlet.2013.10.025

two-fold increase in the ALT level compared with the normal level (El-Beshbishy et al., 2011; Amin and Hamza, 2005).

AZA is rapidly and almost completely converted into 6-mercaptopurine (6-MP) in the liver, and this compound is further metabolized by three enzymatic pathways (Wong et al., 2007; Hisamuddin et al., 2007). The methylation of 6-MP to the inactive 6-methyl mercaptopurine *via* thiopurine methyltransferase (TPMT) is the first pathway. The second pathway involves the metabolization of 6-MP into 6-thiouric acid, which is an inactive metabolite, by xanthine oxidase (XO). The third pathway converts 6-MP into 6-thioinosine 5-monophosphate *via* hypoxanthine guanine phosphoribosyl transferase, and this intermediate is then metabolized into active 6-thioguanine nucleotides. It has been reported that XO has the potential to generate reactive oxygen species (ROS) in human hepatocytes (Petit et al., 2008) and that the oxidation of 6-MP by XO is involved in the AZA-induced liver injury in patients with inflammatory bowel disease (Ansari et al., 2008).

In addition, AZA causes fever and rash, which suggests that inflammation-related mechanisms underlie the AZA-induced liver injury (Jeurissen et al., 1990). However, at present, the involvement of immune- and/or inflammation-related reactions in the AZA-induced liver injury has not been reported. Toll-like receptors (TLR) and the receptors for advanced glycation end products (RAGE), which are expressed on multiple innate immune cells, such as macrophages and dendritic cells, contribute to the activation of the innate immune system (Hennessy et al., 2010; Thornalley, 1998). It was recently reported that damage-associated molecular patterns (DAMPs), such as high-mobility group box 1 (HMGB1) and S100 proteins, which are the ligands of TLR and RAGE, are induced by ROS (Yao and Brownlee, 2010). The relationship between the activation of TLR4 or RAGE and DILI has been reported in acetaminophen- and carbamazepine-induced liver injury (Antoine et al., 2009; Higuchi et al., 2012b), which suggests that the pathogenesis of DILI involves the activation of the inflammatory system. However, only a few studies have investigated the mechanisms of immune- and inflammation-mediated DILI.

Cytokines and chemokines, which result in inflammation or infiltration of lymphocytes into the hepatocytes, are induced through the activation of TLR or RAGE (Lotze et al., 2007). Alternatively, cytokines are secreted by several immune cells, such as macrophages and T cells (Kita et al., 2001; Oo and Adams, 2010). Helper T (Th) cell-mediated immune responses play pivotal roles in the pathogenesis of a variety of human liver disorders (Kita et al., 2001). Th cells are subdivided into Th1, Th2, and Th17 subsets by their unique production of cytokines and characteristic transcription factors. Th1 cells require T-box expressed in T cells (T-bet) and secrete interferon (IFN)-γ. Th2 cells require the presence of GATA-binding domain (GATA)-3 and produce interleukin (IL)-4 and IL-5. Retinoid-related orphan receptor (ROR)-γt is indispensable for the differentiation of Th17 cells, which mainly secrete IL-17 (Kidd, 2003; Steinman, 2007). We previously reported the relationship between Th cell-related factors and the DILI induced by halothane (Kobayashi et al., 2009), α-naphthylisothiocyanate (Kobayashi et al., 2010), dicloxacillin (Higuchi et al., 2011), diclofenac (Yano et al., 2012), carbamazepine (Higuchi et al., 2012b), flutamide (Higuchi et al., 2012a), and methimazole (Kobayashi et al., 2012).

In this study, we established the development of AZA-induced liver injury in wild-type mice and demonstrated that oxidative stress and a set of subsequent inflammation- and immune-related factors are involved in AZA-induced liver injury.

2. Materials and methods

2.1. Chemicals

AZA was purchased from Tokyo Chemical Industry (Tokyo, Japan). Tempol was obtained from Santa Cruz Biotechnology (Santa Cruz, CA). Allopurinol was purchased from Woko Pure Chemical Industries (Osaka, Japan). Eritoran was kindly provided by Eisai Co. (Tokyo, Japan). RNAiso was purchased from Nippon Gene (Tokyo, Japan). ReverTra Ace was obtained from Toyobo (Tokyo, Japan). Random hexamer and SYBR Premix Ex Taq were obtained from Takara (Osaka, Japan). All of the primers were commercially synthesized by Hokkaido System Sciences (Sapporo, Japan). Rabbit polyclonal antibody against myeloperoxidase (MPO) was obtained from DAKO (Carpinteria, CA). The HMGB1 ELISA kit II was purchased from Sino-Test Corporation (Tokyo, Japan). The Fuji DRI-CHEM slides of GPT/ALT-PIII and GOT/AST-PIII that were used to measure the levels of alanine aminotransferase (ALT) and aspartate aminotransferase (AST), respectively, were obtained from Fujifilm (Tokyo, Japan). All of other chemicals were of either analytical grade or the highest commercially available grade.

2.2. AZA administration to mice

Female BALB/cCrSlc mice (8 weeks of age, 18–21 g) were obtained from SLC Japan (Hamamatsu, Japan). The mice were housed in a controlled environment (temperature 25 ± 1 °C, humidity 50 ± 10%, and 12-h light/12-h dark cycle) in the institutional animal facility with access to food and water *ad libitum*. The animals were acclimatized before their use in the experiments. Non-fasting mice were orally (*p.o.*) administered AZA (in corn oil) at a dose of 100, 200, and 300 mg/kg on the appropriate days. The blood and liver were collected 24 h after the last administration. A portion of each excised liver was fixed in 10% formalin neutral buffer solution. The degree of liver injury was assessed by hematoxylin–eosin (H&E) staining. The animal maintenance and treatment were conducted in accordance with the National Institutes of Health Guide for Animal Welfare of Japan, and the protocol was approved by the Institutional Animal Care and Use Committee of Kanazawa University of Japan.

2.3. GSH and GSSG levels

The mouse livers were homogenized in ice-cold 5% sulfosalicylic acid using a glass homogenizer and centrifuged at 8000 × *g* and 4 °C for 10 min. The glutathione (GSH) and glutathione disulfide (GSSG) concentrations in the supernatant were measured as described previously (Tietze, 1969).

2.4. Protein carbonyl contents and SOD activities

Protein carbonyl contents and superoxide dismutase (SOD) activities of liver homogenate were measured using a Protein Carbonyl ELISA kit (Enzo Life Science, Farmingdale, NY) and a Superoxide Dismutase Assay kit (Cayman Chemical, Ann Arbor, MI), respectively.

2.5. Administration of an antioxidant agent

The mice were intraperitoneally (*i.p.*) administered tempol, which is an antioxidant agent (200 mg/kg in PBS) at the same time as the AZA administration (200 mg/kg in corn oil, *p.o.*) during a period of five days. The plasma and liver were collected 24 h after the last AZA administration.

2.6. Administration of a xanthine oxidase inhibitor

The mice were administered allopurinol, which is a xanthine oxidase (XO) inhibitor (30 mg/kg in sterilize PBS, *i.p.*) at the same time as the AZA administration (200 mg/kg in corn oil, *p.o.*) during a period of three days. The plasma was collected 24 h after the last administration.

2.7. Hydrogen peroxide levels

The plasma hydrogen peroxide (H_2O_2) levels were measured using a Hydrogen Peroxide Assay kit (Bio Vision, Milpitas, CA).

2.8. Real-time reverse transcription (RT)-PCR

The RNA from the mouse liver was isolated using RNAiso according to the manufacturer's instructions. The expression levels of TLR2, TLR4, RAGE, S100A8, S100A9, T-bet, GATA-3, ROR-γt, IFN-γ, tumor necrosis factor (TNF)-α, IL-1β, NACHT-LRR-PYD-containing protein 3 (NALP3), and macrophage inflammatory protein (MIP)-2 were quantified by real-time RT-PCR. The primer sequences used in this study are shown in Table 1. For the RT, the total RNA (10 μg) and random hexamer (150 ng) were mixed and incubated at 70 °C for 10 min. The RNA solution was added to a reaction mixture containing 100 units of ReverTra Ace reaction buffer and 0.5 mM dNTPs in a final volume of 40 μl. The reaction mixture was incubated at 30 °C for 10 min, 42 °C for 1 h, and then 98 °C for 10 min to inactivate the enzyme. The real-time RT-PCR was performed using the Mx3000P instrument (Stratagene, La Jolla, CA). The PCR mixture contained 1 μl or 2 μl of template cDNA, SYBR Premix Ex Taq solution, and 8 pmol of the forward and reverse primers. The amplified products were monitored directly by measuring the increase in the intensity of the SYBR Green I dye (Molecular Probes, Eugene, OR).

Table 1
Sequences of primers used for real-time RT-PCR analyses.

Gene		Sequence
TLR2	FP	5′-GAA AAG ATG TCG TTC AAG GAG-3′
	RP	5′-TTG CTG AAG AGG ACT GTT ATG-3′
TLR4	FP	5′-TTC TTC TCC TGC CTG ACA CC-3′
	RP	5′-CCA TGC CAT GCC TTG TCT TC-3′
RAGE	FP	5′-GAA ACT TCT GAT TCC CGA TGG-3′
	RP	5′-GCT CAA CCA ACA GCT GAA TG-3′
S100A8	FP	5′-GAT GGC CAA CAA AGC ACC TT-3′
	RP	5′-TAG ACA TAT CCA GGG ACC CAG-3′
S100A9	FP	5′-GAT GGC CAA CAA AGC ACC TT-3′
	RP	5′-CCT CAA AGC TCA GCT GAT TG-3′
T-bet	FP	5′-CAA GTG GGT GCA GTG TGG AAA G-3′
	RP	5′-TGG AGA GAC TGC AGG ACG ATC-3′
GATA3	FP	5′-GGA GGA CTT CCC CAA GAG CA-3′
	RP	5′-CAT GCT GGA AGG GTG GTG A-3′
ROR-γt	FP	5′-ACC TCC ACT GCC AGC TGT GTG CTG TC-3′
	RP	5′-TCA TTT CTG CAC TTC TGC ATG TAG ACT GTC CC-3′
IFN-γ	FP	5′-GGC CAT CAG CAA CAT AAG C-3′
	RP	5′-TGG ACC ACT CGG ATG AGC TCA-3′
TNF-α	FP	5′-TGT CTC AGC CTC TTC TCA TTC C-3′
	RP	5′-TGA GGG TCT GGG CCA TAG AAC-3′
IL-1β	FP	5′-GTT GAC GGA CCC CAA AAG AT-3′
	RP	5′-CAC ACA CCA GCA GGT TAT CA-3′
NALP3	FP	5′-AGC CTT CCA GGA TCC TCT TC-3′
	RP	5′-CTT GGG CAG CAG TTT CTT TC-3′
MIP-2	FP	5′-AAG TTT GCC TTG ACC CTG AAG-3′
	RP	5′-ATC AGG TAC GAT CCA GGC TTC-3′
GAPDH	FP	5′-AAA TGG GGT GAG GCC GGT-3′
	RP	5′-ATT GCT GAC AAT CTT GAG TGA-3′

FP, forward primer; RP, reverse primer.

2.9. Administration of a TLR4 antagonist

The mice were intravenously (*i.v.*) treated with eritoran (50 μg/mouse in 0.2 ml of sterile saline), which is a TLR4 antagonist (Savov et al., 2005), on fifth day of the AZA administration (200 mg/kg in corn oil, *p.o.*). The blood was collected 24 h after the final administration.

2.10. Immunohistochemical staining of hepatic MPO-positive cells

The infiltration of neutrophils was assessed by immunostaining for MPO. A rabbit polyclonal antibody against MPO was used for the immunohistochemical staining of the liver as previously described by Kumada et al. (2004). Five visual fields at 400× magnification (each with an area of 0.1 mm^2) were randomly selected from each MPO-immunostained specimen, and a picture was taken with a digital camera (D-33E, OLYMPUS, Tokyo).

2.11. Statistical analysis

The data are presented as the mean ± SEM. The statistical analyses between multiple groups were performed using one-way analysis of variance (ANOVA) followed by Tukey's *post hoc* test. The comparisons between two groups were performed using two-tailed Student *t*-test. Differences with a value of $p < 0.05$ were considered statistically significant.

3. Results

3.1. Hepatotoxic effect of AZA in mice

AZA (200 mg/kg, *p.o.*) was administered to female BALB/c mice once daily for a period of six days. The plasma ALT and AST levels were significantly increased in the AZA-treated mice compared with the corn oil-treated and non-treated (NT) mice on days 3, 5, and 6 (Fig. 1A). A dose-dependent increase in the plasma ALT was observed with AZA doses of 100, 200, and 300 mg/kg, which resulted in the maximum plasma ALT levels of approximately 1900, 2500, and 2000 U/l, respectively (Fig. 1B). The repeated administration of AZA at a dose of 300 mg/kg caused high mortality (50% of the mice were dead after six days of AZA administration). We speculated that this high mortality was caused by its immunosuppressive action. A relatively high mortality was also observed after more than seven days and eight days of the administration of 200 mg/kg and a 100 mg/kg AZA, respectively. Based on these data, we selected to administer an AZA dose of 200 mg/kg once daily during a period of six days in the subsequent experiments. No increase in the ALT level was observed in the corn oil-treated mice. The time-dependent changes in hepatotoxicity after the administration of AZA for six days were investigated (Fig. 1C). Twenty-four hours after the final AZA administration, the plasma ALT level showed the maximum level. Histologically, hepatic lobular architecture was mildly distorted and swollen hepatocytes were observed here and there in AZA-treated mice (200 mg/kg for 6 days). Anisocytosis and anisonucleosis of hepatocytes reflected hepatocellular damage and regeneration. Coagulative necrosis of hepatocytes was observed occasionally (Fig. 1D). In sinusoids, lymphocytic infiltration was observed mildly.

3.2. Involvement of oxidative stress in AZA-induced liver injury

The hepatic GSH contents were significantly decreased in AZA-treated mice compared with NT mice and/or corn oil-treated mice on days 1, 3, 5, and 6. The corn oil-treated mice showed no significant change (Fig. 2A). The GSSG levels were significantly increased in AZA-treated mice compared with NT mice and corn oil-treated mice on days 3, 5, and 6. The GSH/GSSG ratio, which is used as an oxidative stress marker, exhibited a similar profile to that obtained with the GSH levels (Fig. 2A). Furthermore, other oxidative stress markers were measured. The hepatic protein carbonyl levels were significantly increased in AZA-treated mice compared with corn oil-treated mice on day 6 (Fig. 2B). SOD, which is the primary ROS detoxification enzyme, catalyze the dismutation of superoxide radicals into molecular oxygen and H_2O_2 (Fridovich, 1989). The SOD activity levels have been used as an oxidative stress marker and are significantly decreased in mice with APAP-induced liver injury (Agarwal et al., 2011). The hepatic SOD activities were significantly decreased in AZA-treated mice compared with NT mice and/or corn oil-treated mice on days 5 and 6 (Fig. 2C). The administration of the antioxidant tempol significantly decreased the plasma ALT levels, as shown by the comparison of the ALT levels in the AZA plus tempol-treated mice and the AZA-treated mice on days 4 and 5 (Fig. 2D). The significantly decreased hepatic SOD activities in the AZA-treated mice were restored by tempol treatment (Fig. 2E).

3.3. Effect of a xanthine oxidase inhibitor in AZA-induced liver injury

We investigated the effect of allopurinol, which is a xanthine oxidase inhibitor, to clarify the involvement of ROS in AZA-induced liver injury. The plasma ALT levels were significantly decreased in the AZA plus allopurinol-treated mice compared with the AZA-treated mice on day 3 (Fig. 3A). The plasma levels of H_2O_2, which is the most stable ROS, were significantly decreased 1 h after the last administration (Fig. 3B).

3.4. Involvement of receptors and ligands from the innate immune system and DAMPs in AZA-induced liver injury

To investigate whether the innate immune system is involved in AZA-induced liver injury, the mRNA expression levels of TLR2, TLR4, RAGE, S100A8, and S100A9 were measured in the liver of AZA-treated mice on days 1, 3, 5, and 6 (Fig. 4A). The mRNA

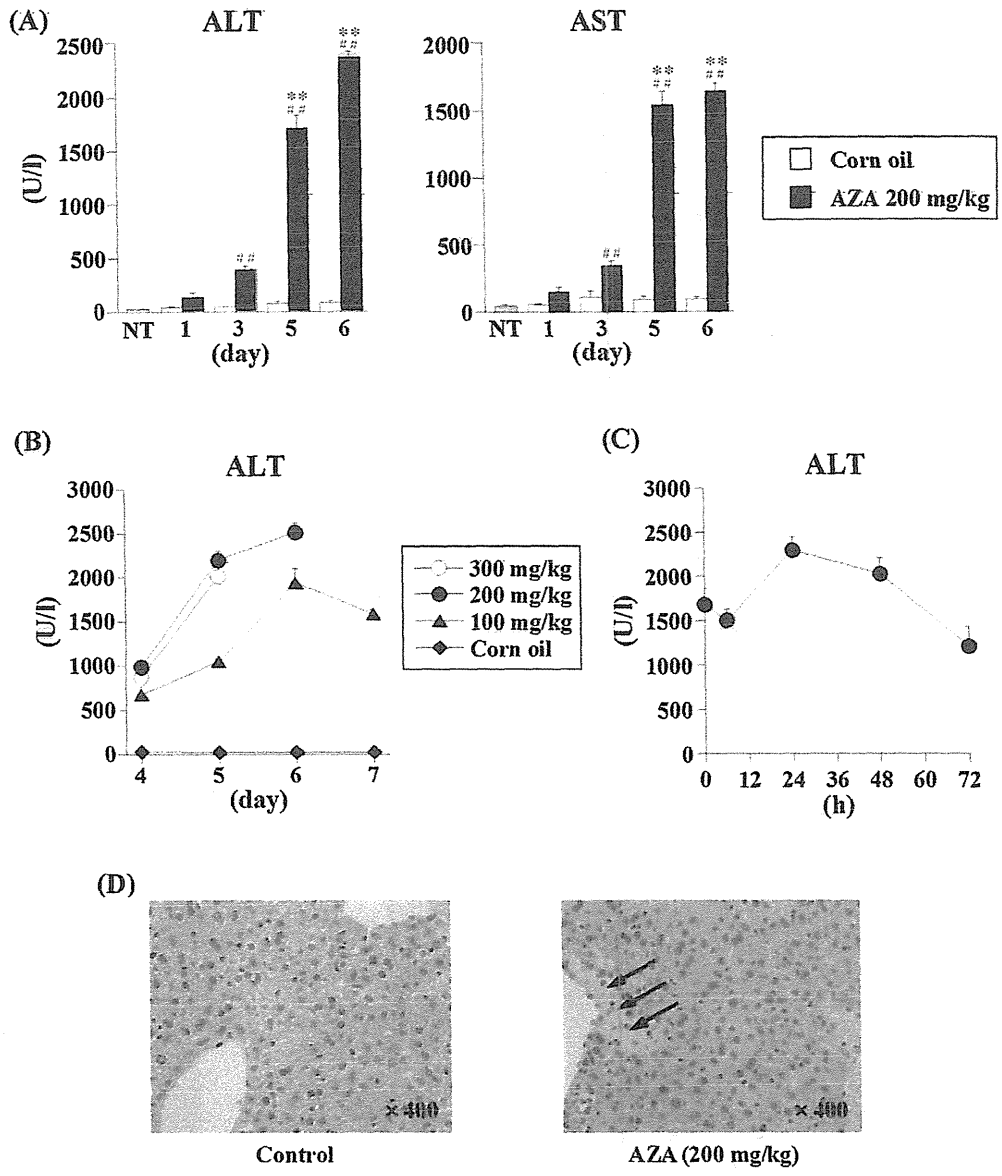

Fig. 1. Dose- and time-dependent changes in the plasma ALT and AST levels and histopathological examination of the liver of AZA-treated mice. (A) The mice were administered AZA (200 mg/kg in 10 ml/kg corn oil, *p.o.*) once daily for six days. Mice that were orally administered corn oil once daily for six days were used as the control. The plasma ALT and AST levels were measured 24 h after AZA was administered for period of one, three, five, and six days. (B) The mice were administered AZA at a dose of 100, 200, and 300 mg/kg once daily for seven, six, and five days, respectively. The plasma ALT levels were measured 24 h after AZA was administered for period of four through seven days. (C) The mice were administered AZA (200 mg/kg in corn oil, *p.o.*) once daily for six days. The plasma ALT levels were measured 0, 6, 24, 48, and 72 h after the last administration. The data represent the mean ± SEM ($n = 4$–6). **,##Significantly different compared with the non-treated (NT) mice (**$p < 0.01$) and control mice (##$p < 0.01$). (D) The liver sections from the AZA-treated mice (200 mg/kg in corn oil, *p.o.*, once daily for six days) were strained with H&E. The black arrows indicate necrotic cells.

expression level of TLR2 was significantly increased in AZA-treated mice compared with NT mice and/or corn oil-treated mice on days 3, 5, and 6. The mRNA expression level of TLR4 was significantly increased in AZA-treated mice compared with NT mice and corn oil-treated mice on days 5 and 6. The mRNA expression levels of RAGE, S100A8, and S100A9 were significantly increased in AZA-treated mice compared with NT mice and/or corn oil-treated mice on day 5. The HMGB1 protein is secreted from activated immune cells and is also passively released from necrotic cells (Wang et al., 2004). The release of HMGB1 protein is not correlated with the increased expression of hepatic HMGB1 mRNA. Thus, the plasma concentration of HMGB1 protein was measured using ELISA, and the results showed a significant increase in the amount of HMGB1 protein in AZA-treated mice compared with NT mice and corn oil-treated mice on day 6 (Fig. 4B). To investigate whether the TLR4 signaling cascade is involved in AZA-induced liver injury, mice were administered eritoran, a TLR4 antagonist, on day 5. The plasma ALT levels were significantly decreased in the AZA plus eritoran-treated mice compared with the AZA-treated mice (Fig. 4C).

3.5. Expression of T cell transcription factors and involvement of the inflammatory response in AZA-induced liver injury

To investigate the involvement of Th cells and the inflammatory response in AZA-induced liver injury, we measured the hepatic mRNA levels of immune-related transcription factors (T-bet, GATA-3, and ROR-γt) and inflammatory-related factors (INF-γ, TNF-α, IL-1β, NAPL3, and MIP-2; Fig. 5A). The mRNA expression levels

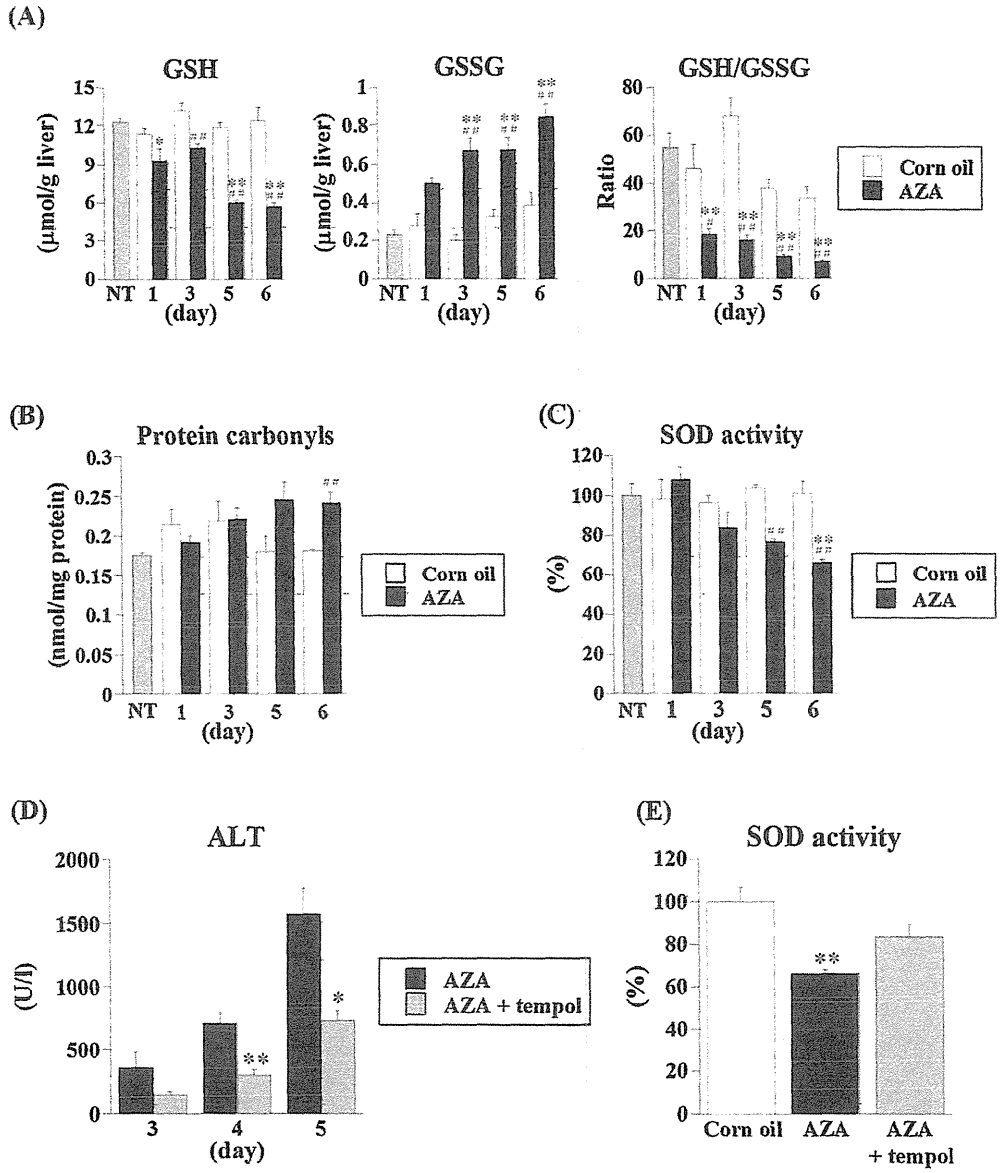

Fig. 2. Time-dependent changes in the hepatic GSH and GSSG levels and the GSH/GSSG ratio, the effect of antioxidants, and the oxidative stress marker levels in AZA-induced liver injury. The mice were administered AZA (200 mg/kg in corn oil, *p.o.*) once daily for six days. Mice that were orally administered corn oil were used as the control. The hepatic GSH and GSSG levels and the GSH/GSSG ratio (A), protein carbonyls (B), and SOD activities (C) were measured 24 h after AZA was administered for period of 1, 3, 5, and 6 days. The data represent the mean ± SEM ($n = 4$–6). *,**,#,##Significantly different compared with the non-treated (NT) mice (*$p < 0.05$, **$p < 0.01$) and control mice (#$p < 0.05$, ##$p < 0.01$). (D) The mice were administered tempol (200 mg/kg in sterilize PBS, *i.p.*) and AZA (200 mg/kg in corn oil, *p.o.*) simultaneously for a period of up to five days. The plasma ALT levels were measured 24 h after AZA was administered for three, four, and five days. The data represent the mean ± SEM ($n = 4$–6). *,**Significantly different compared with the AZA-treated mice (*$p < 0.05$, **$p < 0.01$). (E) The mice were administered tempol (200 mg/kg in sterilize PBS, *i.p.*) and/or AZA (200 mg/kg in corn oil, *p.o.*) simultaneously for five days. The hepatic SOD activities were measured 24 h after the last administration. The data represent the mean ± SEM ($n = 4$–6). **Significantly different compared with the corn oil-treated mice (**$p < 0.01$).

of TNF-α, IL-1β, and MIP-2 were significantly increased in AZA-treated mice compared with NT mice and/or corn oil-treated mice on days 5 and 6. The mRNA expression levels of T-bet and NALP3 were significantly increased in AZA-treated mice compared with NT mice and/or corn oil-treated mice on day 5. However, the expression levels of GATA-3, ROR-γt, and INF-γ were not significantly altered. Neutrophils were detected by anti-MPO antibody in immunohistochemistry. Small aggregation of neutrophils was observed here and there in hepatic parenchyma of AZA-treated mice (200 mg/kg for 6 days), while it was not observed in the corn oil-treated mice (Fig. 5B).

4. Discussion

AZA is reported to cause various adverse reactions and leads to liver injury in a small number of patients who are prescribed AZA (Marinaki et al., 2004; Takatsu et al., 2009). The mechanisms of AZA-induced liver injury have not been adequately clarified. The hepatotoxicity of AZA (less than two-fold higher than the normal level of ALT) in rats has been reported to be protected by green tea polyphenols (El-Beshbishy et al., 2011) and herbal plants (Amin and Hamza, 2005). In addition, extra-hepatic manifestations, such as fever and rash, have been reported in patients with

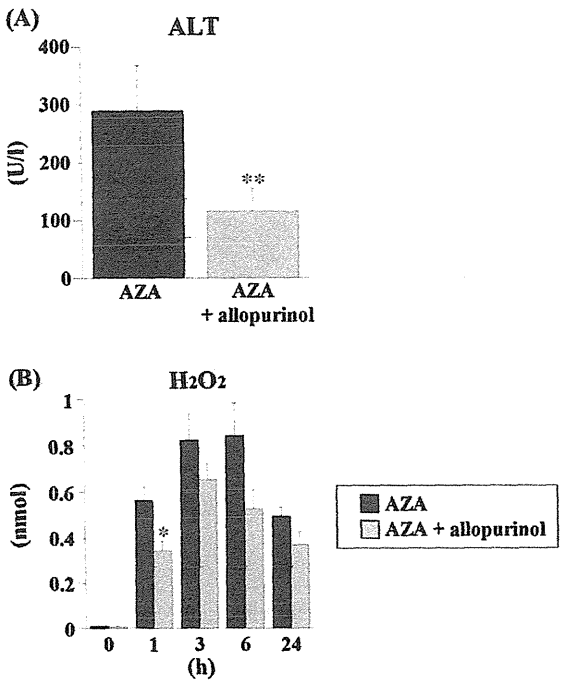

Fig. 3. Effect of a xanthine oxidase inhibitor on the plasma ALT levels and time-dependent changes in the plasma H_2O_2 levels in mice with AZA-induced liver injury. (A) The mice were administered AZA (200 mg/kg in corn oil, *p.o.*) and allopurinol (30 mg/kg in sterilize PBS, *i.p.*) simultaneously for three days. The plasma ALT levels were measured 24 h after the last administration. (B) The plasma H_2O_2 levels were measured 1, 3, 6, and 24 h after the last administration. The data represent the mean ± SEM ($n = 4$–5). *,**Significantly different compared with AZA-treated mice (*$p < 0.05$, **$p < 0.01$).

AZA-induced liver injury (Jeurissen et al., 1990). Although this observation suggests that immunological mechanisms underlie the pathogenesis of AZA-induced liver injury, the involvement of immune- and inflammation-related factors in AZA-induced liver injury *in vivo* has never been reported. In this study, we established a mouse model of AZA-induced liver injury and investigated the involvement of both oxidative stress and immunological responses in AZA-induced liver injury.

First, we investigated the effect of different AZA dosing program. Because AZA is administered orally in clinical practice, we administered AZA orally to mice. The dose of 200 mg/kg (*p.o.*, approximately one-twelfth of the murine oral LD50) was adopted, and the plasma ALT levels were measured 24 h after the last AZA administration, which is the time point that showed the highest ALT levels (Fig. 1B and C). Using the selected dosing program, the ALT and AST levels started to increase on day 3 and were markedly higher on days 5 and 6 (Fig. 1A). Furthermore, liver injury was confirmed through the histological evaluation of liver sections obtained from mice six days after the last AZA administration (Fig. 1D). We regarded the increase in the plasma ALT levels on day 3 as the initiation phase of AZA-induced liver injury and the higher increases on days 5 and 6 as the exacerbation phase. Clinical reports have shown that acute and chronic liver injury develops within weeks-years and 1–5 years after the initiation of AZA treatment, respectively. Liver injury has been recognized in 2% of AZA-treated patients. To definitely induce liver injury, we administered an AZA dose that was 40-fold higher than the clinical dose.

Hepatic GSH is consumed during the metabolism of AZA into 6-MP catalyzed by glutathione S-transferases. GSH is responsible for ROS scavenging and is converted into GSSG. Therefore, the decrease in GSH and the increase in GSSG induced by AZA administration may be caused by the AZA metabolism and ROS scavenging (Fig. 2A). The low GSH/GSSG ratio suggests that the AZA-treated mice are vulnerable to oxidative stress. The increase of hepatic protein carbonyl levels (Fig. 2B), the decrease of hepatic SOD activities (Fig. 2C), and the suppression of the increased plasma ALT levels by the antioxidant tempol (Fig. 2D) in AZA-treated mice indicate the involvement of oxidative stress in AZA-induced liver injury *in vivo* in mice. The decreased SOD activities in the AZA-treated mice were recovered by tempol administration (Fig. 2E), which suggests that tempol ameliorates the AZA-induced liver injury through the suppression of oxidative stress. It is interesting to note that GSH/GSSG ratio was decreased by AZA treatment from day 1, when ALT level was not changed. In addition, content of hepatic protein carbonyl and SOD activities showed the increasing and the decreasing tendency, respectively from day 3. These results suggested that the oxidative stress is involved in AZA-induced liver injury from early stage.

The metabolic conversion of 6-MP into 6-thiouric acid *via* XO, which is a critical source of ROS, potentially leads to hepatotoxicity. We inhibited XO using allopurinol, which is an inhibitor of XO, to investigate the involvement of XO in AZA-induced liver injury. The increased plasma ALT levels in AZA-treated mice were suppressed by allopurinol (Fig. 3A). An allopurinol dose of 30 mg/kg was sufficient to inhibit the XO activity in mice, as reported previously (Zhao et al., 2006). To investigate whether ROS was decreased by allopurinol, the plasma H_2O_2 levels were measured on day 3. The results show that allopurinol suppressed the plasma H_2O_2 levels (Fig. 3B). Although a significant change was recognized only 1 h after the last AZA administration, the plasma H_2O_2 levels in the allopurinol-treated mice tended to decrease over a period of 24 h. These data suggest that XO-induced ROS are involved in AZA-induced liver injury in mice. However, this effect of allopurinol was not observed on days 5 and 6 (data not shown), which suggests that the ROS generation through the AZA metabolism may be involved only in the initiation phase of liver injury.

It has been reported that ROS induces the expression of TLR4 ligands and RAGE (Yao and Brownlee, 2010). We thus investigated whether these factors are involved in AZA-induced liver injury. The hepatic mRNA levels and the plasma protein levels of receptors (TLR2, TLR4, and RAGE) and their ligands (S100A8, S100A9, and HMGB1) were significantly increased in AZA-induced liver injury (Fig. 4A and B), particularly during the late phase (on days 5 and 6). Therefore, we administered eritoran, a TLR4 antagonist, to mice on day 5 of AZA administration. The protective effect of eritoran for DILI was previously investigated in detail and was reported in carbamazepine-induced liver injury in mice (Higuchi et al., 2012b). In this study, we adapted the same dosing and timing schedule in AZA administration. A significant decrease in the plasma ALT levels was found in the AZA plus eritoran-treated mice compared with the AZA-treated mice (Fig. 4C), which indicates that the activation of the innate immune system contributes to the exacerbation phase of AZA-induced liver injury. However, the protective effect was relatively modest, which suggested the TLR4 signaling was partly involved in AZA-induced liver injury.

The hepatic mRNA levels of T cell-related factors were not significantly changed by AZA administration (Fig. 5A). The expression level of T-bet, which is a transcription factor of Th1 cells, was significantly increased on day 5. However, the expression level of IFN-γ, a pro-inflammatory cytokine secreted by Th1 cells, was not changed. In addition, changes in the plasma protein levels of IL-4 and IL-17, which are pro-inflammatory cytokines secreted by Th2 and Th17 cells, respectively, were not detected (data not shown). These results suggest that the pharmacological effect of AZA, *i.e.*, immune suppression, might inhibit the response of T cells. Thus, these T cell-related factors are not likely to be involved in AZA-induced liver injury.

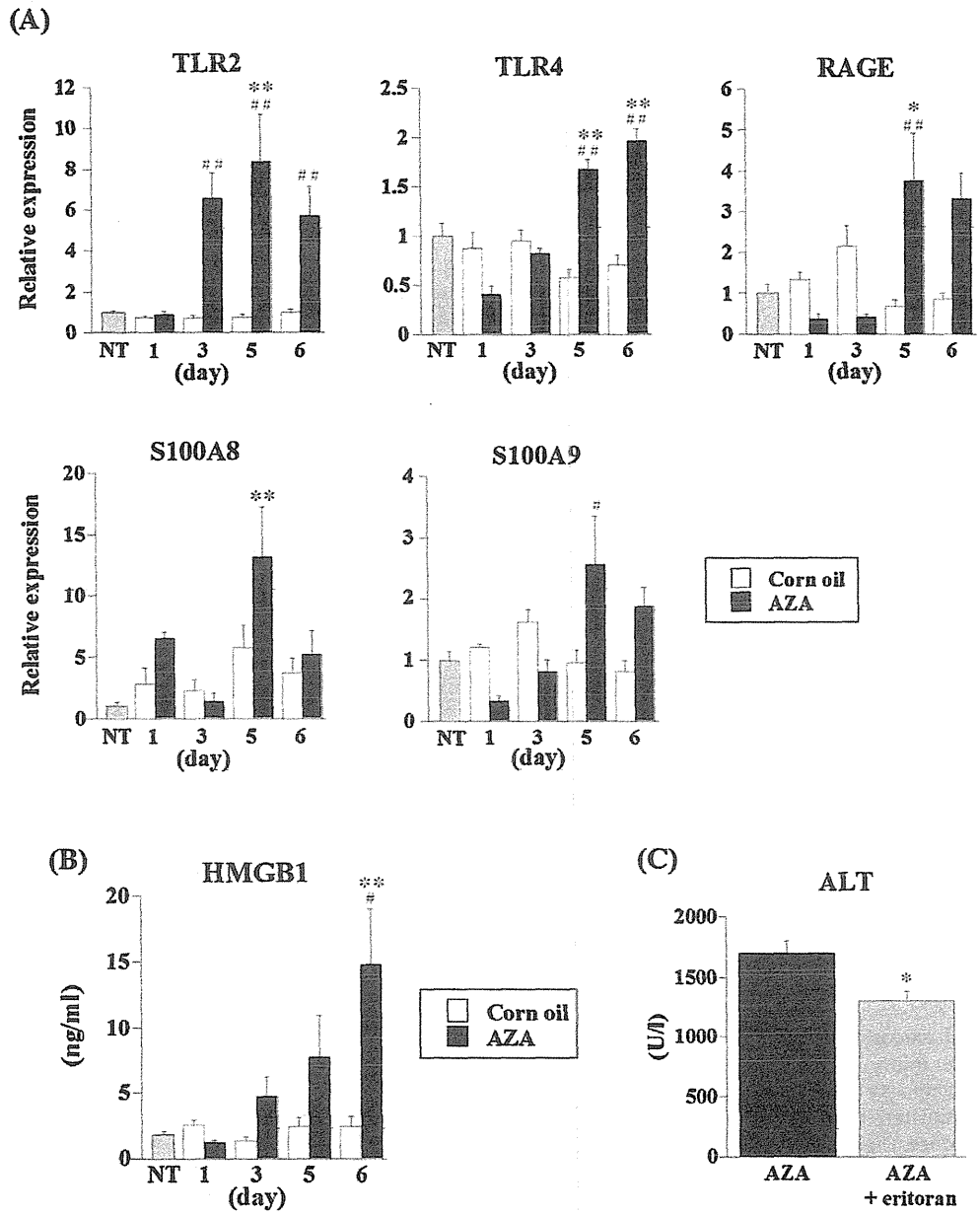

Fig. 4. Time-dependent changes in the hepatic mRNA expression levels of DAMP-related genes and the plasma HMGB1 protein levels and effect of a TLR4 antagonist on the plasma ALT levels in mice with AZA-induced liver injury. (A and B) The mice were administered AZA (200 mg/kg in corn oil, *p.o.*) once daily for six days. Mice that were orally administered corn oil were used as the control. The hepatic mRNA expression levels of DAPM-related genes and the plasma HMGB1 protein levels were measured 24 h after AZA was administered for one, three, five, and six days. The data represent the mean ± SEM ($n = 4$–6). *,**,#,##Significantly different compared with non-treated (NT) mice ($^*p < 0.05$, $^{**}p < 0.01$) and corn oil-treated mice ($\#p < 0.05$, $\#\#p < 0.01$). (C) The mice were administered AZA (200 mg/kg in corn oil, *p.o.*) once daily for five days; and eritoran (50 μg/mouse in 0.2 ml sterile saline, *i.v.*) was administered with the last AZA administration (on day 5). The plasma ALT levels were measured 24 h after the last administration. The data represent the mean ± SEM ($n = 4$–6). *Significantly different compared with AZA-treated mice ($^*p < 0.05$).

By contrast, the hepatic mRNA levels of inflammation-related factors (TNF-α, IL-1β, MIP-2, and NALP3) were significantly increased in the AZA-treated mice (Fig. 5A). TNF-α and IL-1β are pro-inflammatory cytokines produced by a variety of immune cells, such as macrophages, mast cells, and dendritic cells (Tracey, 1994; Arend et al., 2008). MIP-2 is a chemokine released by macrophages. IL-1β and MIP-2 recruit leukocytes, particularly neutrophils, into the liver (Bajt et al., 2001). The NALP3 inflammasome mediates the processing of IL-1β, which is activated by ROS and DAMPs (Agostini et al., 2004). The infiltration of neutrophils was confirmed by anti-MPO straining (Fig. 5B). These data suggest the involvement of the inflammatory response in the exacerbation phase of AZA-induced liver injury.

Based on the presented data, AZA-induced liver injury might be caused by oxidative stress through the generation of ROS during the initiation phase of hepatotoxicity. In contrast, inflammation-related factors might be involved in the exacerbation phase. In other words, the injury of hepatocytes by oxidative stress might be the first step of AZA-induced liver injury, and this step is likely followed by the inflammatory response induced by the DAMPs released by necrotic hepatocytes. The putative mechanism of AZA-induced liver injury is summarized in Fig. 6.

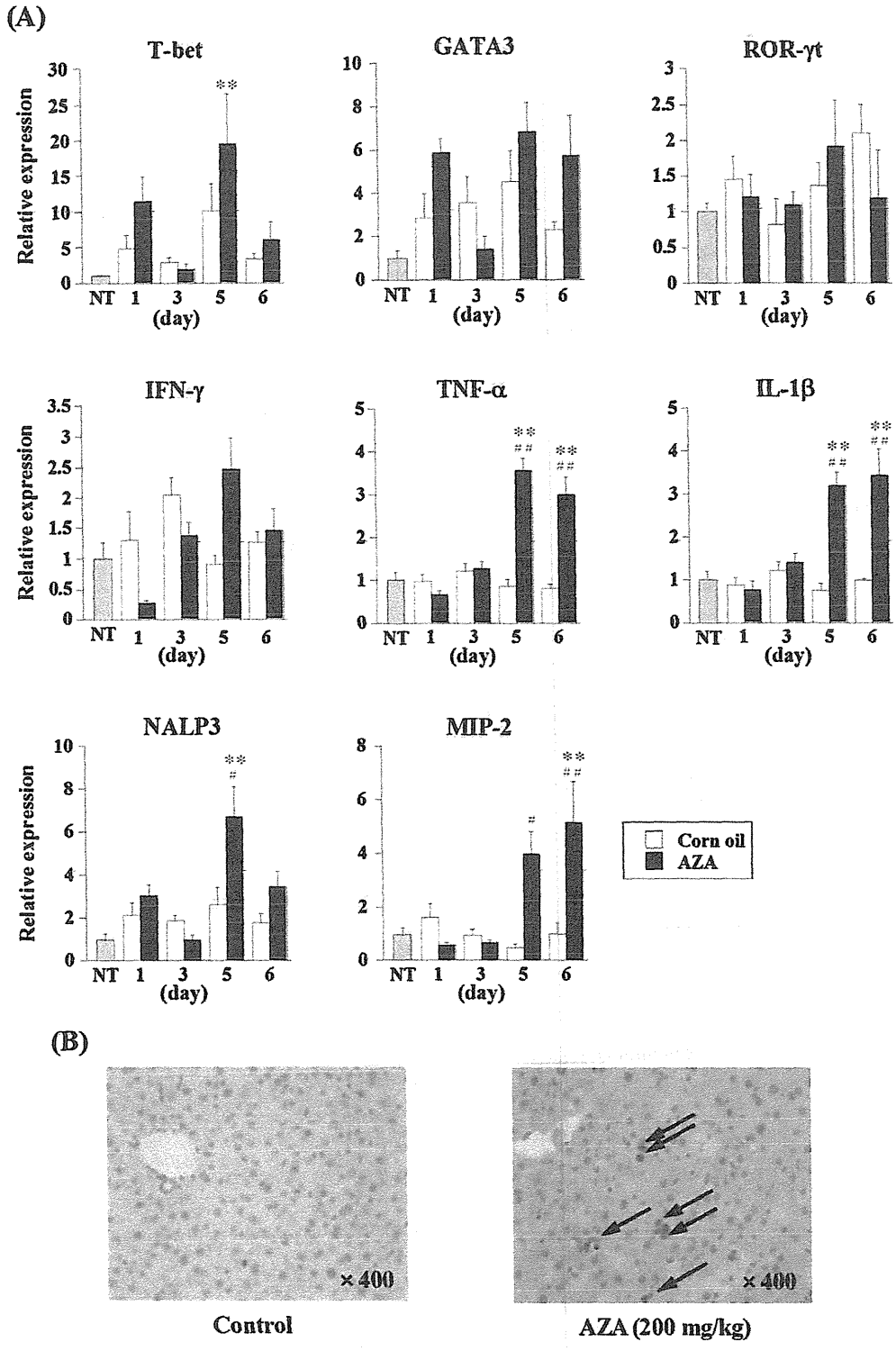

Fig. 5. Time-dependent changes in the hepatic mRNA expression levels of T-cell transcription factors and inflammation-related factors. (A) AZA was administered using the dosing schedule described in Fig. 4. (A and B) The data represent the mean ± SEM ($n = 4$–6). *,**,#,##Significantly different compared with non-treated (NT) mice (*$p < 0.05$, **$p < 0.01$) and corn oil-treated mice (#$p < 0.05$, ##$p < 0.01$). (B) The mononuclear cell infiltration was assessed by immunostaining for MPO. The black arrows indicate MPO-positive cells.

It is hypothesized that multiple mechanisms cause AZA-induced liver injury. A case study suggested the contribution of genetic factors because two of three patients who developed AZA-induced liver injury possessed similar HLA haplotypes (Jeurissen et al., 1990). Alternatively, TPMT is an enzyme that mediates the methylation of 6-MP. High TPMT activity and methylated metabolites levels have been correlated with hepatotoxicity in humans (Dubinsky et al., 2002; Van Asseldonk et al., 2012), which suggests that reactive metabolites may be involved in AZA-induced liver injury. These factors should be considered in future studies

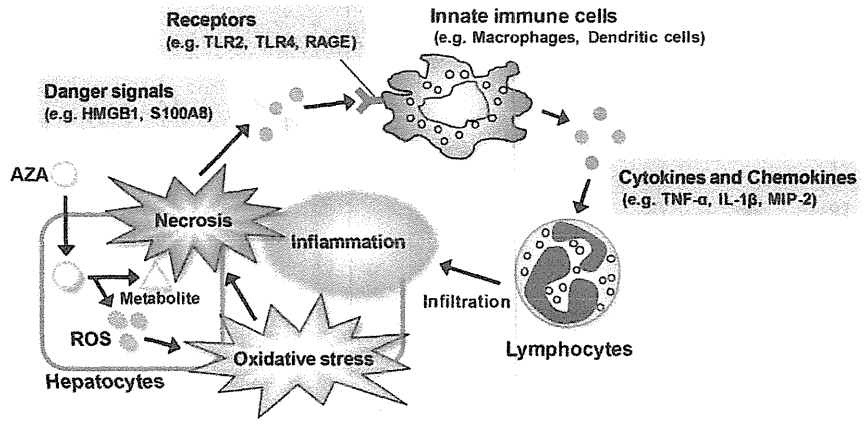

Fig. 6. The putative mechanism of AZA-induced liver injury. During metabolism of AZA in hepatocytes, ROS are produced. ROS-induced oxidative stress causes necrosis of hepatocytes. Danger signals released from hepatocytes activate innate immune cells *via* their receptors. Activated innate immune cells lead to the secretion of cytokines and chemokines, which resulted in inflammation in the liver.

to further clarify the mechanism of AZA-induced liver injury in humans.

In conclusion, we successfully established a mouse model of AZA-induced liver injury and demonstrated the involvement of oxidative stress, the generation of ROS, and inflammation-related factors in AZA-induced liver injury. Based on our findings, inflammation-related factors are associated with the exacerbation phase of AZA-induced liver injury. In contrast, oxidative stress and ROS generation may affect the initiation phase of AZA-induced liver injury. Furthermore, we showed the potential effectiveness of allopurinol, antioxidant agents, and TLR4 inhibitors for the treatment of AZA-induced liver injury. These finding may provide insight into the mechanisms of DILI.

Funding

This study was funded by Health and Labor Sciences Research Grants from the Ministry of Health, Labor, and Welfare of Japan (H23-BIO-G001).

Conflict of interest

None of the authors have any conflicts of interest related to this manuscript.

References

Agarwal, R., MacMillan-Crow, L.A., Rafferty, T.M., Saba, H., Roberts, D.W., Fifer, E.K., James, L.P., Hinson, J.A., 2011. Acetaminophen-induced hepatotoxicity in mice occurs with inhibition of activity and nitration of mitochondrial manganese superoxide dismutase. J. Pharmacol. Exp. Ther. 337, 110–116.

Agostini, L., Martinon, F., Burns, K., McDermott, M.F., Hawkins, P.N., Tschopp, J., 2004. NALP3 forms an IL-1β-processing inflammasome with increased activity in Muckle-Wells autoinflammatory disorder. Immunity 20, 319–325.

Aithal, G.P., 2011. Hepatotoxicity related to antirheumatic drugs. Nat. Rev. Rheumatol. 7, 139–150.

Amin, A., Hamza, A.A., 2005. Hepatoprotective effects of Hibiscus, Rosmarinus and Salvia on azathioprine-induced toxicity in rats. Life Sci. 77, 266–278.

Ansari, A., Elliott, T., Baburajan, B., Mayhead, P., O'Donohue, J., Chocair, P., Sanderson, J., Duley, J., 2008. Long-term outcome of using allopurinol co-therapy as a strategy for overcoming thiopurine hepatotoxicity in treating inflammatory bowel disease. Aliment. Pharmacol. Ther. 28, 734–741.

Antoine, D.J., Williams, D.P., Kipar, A., Jenkins, R.E., Regan, S.L., Sathish, J.G., Kitteringham, N.R., Park, B.K., 2009. High-mobility group box-1 protein and keratin-18, circulating serum proteins informative of acetaminophen-induced necrosis and apoptosis in vivo. Toxicol. Sci. 112, 521–531.

Arend, W.P., Palmer, G., Gabay, C., 2008. IL-1, IL-18, and IL-33 families of cytokines. Immunol. Rev. 223, 20–38.

Bajt, M.L., Farhood, A., Jaeschke, H., 2001. Effects of CXC chemokines on neutrophil activation and sequestration in hepatic vasculature. Am. J. Physiol. Gastrointest. Liver Physiol. 281, G1188–G1195.

Dejaco, C., Mittermaier, C., Reinisch, W., Gasche, C., Waldhoer, T., Strohmer, H., Moser, G., 2003. Azathioprine treatment and male fertility in inflammatory bowel disease. Gastroenterology 121, 1048–1053.

Dubinsky, M.C., 2004. Azathioprine, 6-mercaptopurine in inflammatory bowel disease: pharmacology, efficacy and safety. Clin. Gastroenterol. Hepatol. 2, 731–743.

Dubinsky, M.C., Yang, H., Hassard, P.V., Seidman, E.G., Kam, L.Y., Abreu, M.T., Targan, S.R., Vasiliauskas, E.A., 2002. 6-MP metabolite profiles provide a biochemical explanation for 6-MP resistance in patients with inflammatory bowel disease. Gastroenterology 122, 904–915.

El-Beshbishy, H.A., Tork, O.M., El-Bab, M.F., Autifi, M.A., 2011. Antioxidant and anti-apoptotic effects of green tea polyphenols against azathioprine-induced liver injury in rats. Pathophysiology 18, 125–135.

Fridovich, I., 1989. Superoxide dismutases. An adaptation to a paramagnetic gas. J. Biol. Chem. 264, 7761–7764.

Hennessy, E.J., Parker, A.E., O'Neill, L.A., 2010. Targeting Toll-like receptors: emerging therapeutics. Nat. Rev. Drug. Discov. 9, 293–307.

Higuchi, S., Kobayashi, M., Yano, A., Tsuneyama, K., Fukami, T., Nakajima, M., Yokoi, T., 2012a. Involvement of Th2 cytokines in the mouse model of flutamide-induced acute liver injury. J. Appl. Toxicol. 32, 815–822.

Higuchi, S., Kobayashi, M., Yoshikawa, Y., Tsuneyama, K., Fukami, T., Nakajima, M., Yokoi, T., 2011. IL-4 mediates dicloxacillin-induced liver injury in mice. Toxicol. Lett. 200, 139–145.

Higuchi, S., Yano, A., Takai, S., Tsuneyama, K., Fukami, T., Nakajima, M., Yokoi, T., 2012b. Metabolic activation and inflammation reactions involved in carbamazepine-induced liver injury. Toxicol. Sci. 130, 4–16.

Hisamuddin, I.M., Wehbi, M.A., Yang, V.W., 2007. Pharmacogenetics and diseases of the colon. Curr. Opin. Gastroenterol. 23, 60–66.

Holt, M.P., Ju, C., 2006. Mechanisms of drug-induced liver injury. AAPS J. 8, 48–54.

Jeurissen, M.E., Boerbooms, A.M., van de Putte, L.B., Kruijsen, M.W., 1990. Azathioprine induced fever, chills, rash, and hepatotoxicity in rheumatoid arthritis. Ann. Rheum. Dis. 49, 25–27.

Kidd, P., 2003. Th1/Th2 balance: the hypothesis, its limitations, and implications for health and disease. Altern. Med. Rev. 8, 223–246.

Kita, H., Mackay, I.R., Van De Water, J., Gershwin, M.E., 2001. The lymphoid liver: considerations on pathways to autoimmune injury. Gastroenterology 120, 1485–1501.

Kobayashi, E., Kobayashi, M., Tsuneyama, K., Fukami, T., Nakajima, M., Yokoi, T., 2009. Halothane-induced liver injury is mediated by interleukin-17 in mice. Toxicol. Sci. 111, 302–310.

Kobayashi, M., Higuchi, S., Ide, M., Nishikawa, S., Fukami, T., Nakajima, M., Yokoi, T., 2012. Th2 cytokine-mediated methimazole-induced acute liver injury in mice. J. Appl. Toxicol. 32, 823–833.

Kobayashi, M., Higuchi, S., Mizuno, K., Tsuneyama, K., Fukami, T., Nakajima, M., Yokoi, T., 2010. Interleukin-17 is involved in α-naphthylisothiocyanate-induced liver injury in mice. Toxicology 275, 50–57.

Kumada, T., Tsuneyama, K., Hatta, H., Ishizawa, S., Takano, Y., 2004. Improved 1-h rapid immunostaining method using intermittent microwave irradiation: practicability based on 5 years application in Toyama Medical and Pharmaceutical University Hospital. Mod. Pathol. 17, 1141–1149.

Lotze, M.T., Zeh, H.J., Rubartelli, A., Sparvero, L.J., Amoscato, A.A., Washburn, N.R., Devera, M.E., Liang, X., Tor, M., Billiar, T., 2007. The grateful dead: damage-associated molecular pattern molecules and reduction/oxidation regulate immunity. Immunol. Rev. 220, 60–81.

Maltzman, J., Koretzky, G., 2003. Azathioprine: old drug new actions. J. Clin. Invest. 111, 1122–1124.

Marinaki, A.M., Ansari, A., Duley, J.A., Arenas, M., Sumi, S., Lewis, C.M., Shobowale-Bakre, el-M., Escuredo, E., Fairbanks, L.D., Sanderson, J.D., 2004. Adverse drug

reactions to azathioprine therapy are associated with polymorphism in the gene encoding inosine triphosphate pyrophosphatase (ITPase). Pharmacogenetics 14, 181–187.

Oo, Y.H., Adams, D.H., 2010. The role of chemokines in the recruitment of lymphocytes to the liver. J. Autoimmun. 34, 45–54.

Petit, E., Langouet, S., Akhdar, H., Nicolas-Nicolaz, C., Guillouzo, A., Morel, F., 2008. Differential toxic effects of azathioprine, 6-mercaptopurine and 6-thioguanine on human hepatocytes. Toxicol. In Vitro 22, 632–642.

Savov, J.D., Brass, D.M., Lawson, B.L., McElvania-Tekippe, E., Walker, J.K., Schwartz, D.A., 2005. Toll-like receptor 4 antagonist (E5564) prevents the chronic airway response to inhaled lipopolysaccharide. Am. J. Physiol. Lung Cell Mol. Physiol. 289, L329–L337.

Steinman, L., 2007. A brief history of Th17, the first major revision in the Th1/Th2 hypothesis if T cell-mediated tissue damage. Nat. Rev. Med. 13, 139–145.

Takatsu, N., Matsui, T., Murakami, Y., Ishihara, H., Hisabe, T., Nagahama, T., Maki, S., Beppu, T., Takaki, Y., Hirai, F., Yao, K., 2009. Adverse reactions to azathioprine cannot be predicted by thiopurine S-methyltransferase genotype in Japanese patients with inflammatory bowel disease. J. Gastroenterol. Hepatol. 24, 1258–1264.

Thornalley, P.J., 1998. Cell activation by glycated proteins. AGE receptors, receptor recognition factors and functional classification of AGEs. Cell. Mol. Biol. 44, 1013–1023.

Tietze, F., 1969. Enzymatic method for quantitative determination of nanogram amounts of total and oxidized glutathione: applications to mammalian blood and other tissues. Anal. Biochem. 27, 502–522.

Tracey, K.J., 1994. Tumor necrosis factor-α. In: Thomson, A. (Ed.), The Cytokine Handbook. Academic Press, London, pp. 289–304.

Van Asseldonk, D.P., Seinen, M.L., De Boer, N.K., Van Bodegraven, A.A., Mulder, C.J., 2012. Hepatotoxicity associated with 6-methyl mercaptopurine formation during azathioprine and 6-mercaptopurine therapy does not occur on the short-term during 6-thioguanine therapy in IBD treatment. J. Crohns Colitis 6, 95–101.

Wang, H., Yang, H., Tracey, K.J., 2004. Extracellular role of HMGB1 in inflammation and sepsis. J. Intern. Med. 255, 320–331.

Wong, D.R., Derijks, L.J., den Dulk, M.O., Gemmeke, E.H., Hooymans, P.M., 2007. The role of xanthine oxidase in thiopurine metabolism: a case report. Ther. Drug Monit. 29, 845–848.

Yano, A., Higuchi, S., Tsuneyama, K., Fukami, T., Nakajima, M., Yokoi, T., 2012. Involvement of immune-related factors in diclofenac-induced acute liver injury in mice. Toxicology 293, 107–114.

Yao, D., Brownlee, M., 2010. Hyperglycemia-induced reactive oxygen species increase expression of the receptor for advanced glycation end products (RAGE) and RAGE ligands. Diabetes 59, 249–255.

Zhao, X., Zhu, J.X., Mo, S.F., Pan, Y., Kong, L.D., 2006. Effects of cassia oil on serum and hepatic uric acid levels in oxonate-induced mice and xanthine dehydrogenase and xanthine oxidase activities in mouse liver. J. Ethnopharmacol. 103, 357–365.

Biochemical Pharmacology 87 (2014) 660–667

Contents lists available at ScienceDirect

Biochemical Pharmacology

journal homepage: www.elsevier.com/locate/biochempharm

Epigenetic regulation of the tissue-specific expression of human UDP-glucuronosyltransferase (UGT) 1A10

Shingo Oda, Tatsuki Fukami, Tsuyoshi Yokoi [1], Miki Nakajima *

Drug Metabolism and Toxicology, Faculty of Pharmaceutical Sciences, Kanazawa University, Kakuma-machi, Kanazawa 920-1192, Japan

ARTICLE INFO

Article history:
Received 18 September 2013
Accepted 4 November 2013
Available online 14 November 2013

Keywords:
Epigenetics
DNA methylation
Tissue-specific regulation
UDP-glucuronosyltransferase

ABSTRACT

Human UDP-glucuronosyltransferase (UGT) 1A10 is not expressed in the liver; however, UGT1A10 is highly expressed in the intestine, contributing to presystemic first-pass metabolism. Earlier studies revealed that hepatocyte nuclear factor (HNF) 1α and Sp1, as well as an intestine-specific transcription factor, caudal type homeobox (Cdx) 2, are involved in the constitutive expression of UGT1A10. However, why UGT1A10 is not expressed in the liver, where HNF1α and Sp1 are abundantly expressed, is unknown. In this study, we sought to elucidate the mechanism, focusing on epigenetic regulation. Bisulfite sequence analysis revealed that the CpG-rich region (−264 to +117) around the *UGT1A10* promoter was hypermethylated (89%) in hepatocytes, whereas the *UGT1A10* promoter was hypomethylated (11%) in the epithelium of the small intestine. A luciferase assay revealed that the methylation of the *UGT1A10* promoter by *SssI* methylase abrogated transactivity even with overexpressed Cdx2 and HNF1α. The *UGT1A10* promoter was highly methylated (86%) in liver-derived HuH-7 cells, where UGT1A10 is not expressed. In contrast, the *UGT1A10* promoter was hardly methylated (19%) in colon-derived LS180 cells, where UGT1A10 is expressed. Treatment with 5-aza-2′-deoxycitidine (5-Aza-dC), an inhibitor of DNA methylation, resulted in an increase in UGT1A10 expression only in HuH-7 cells. Moreover, overexpression of HNF1α and Cdx2 further increased UGT1A10 expression only in the presence of 5-Aza-dC. Collectively, we found that DNA hypermethylation would interfere with the binding of HNF1α and Cdx2, resulting in the defective expression of UGT1A10 in human liver. Thus, epigenetic regulation is one of the mechanisms that determine the tissue-specific expression of UGT1A10.

© 2013 Elsevier Inc. All rights reserved.

1. Introduction

UDP-Glucuronosyltransferases (UGTs) catalyze the glucuronidation of a variety of endogenous and exogenous compounds. In humans, there are 19 functional UGT enzymes, which are classified into three subfamilies: UGT1A, UGT2A, and UGT2B [1]. The *UGT1A* genes, which are located on chromosome 2q37, contain multiple unique first exons and common exons 2–5 and encode nine kinds of functional UGT1A enzymes [2]. The *UGT2* genes, which are located on chromosome 4q13, encode three UGT2A and seven UGT2B functional enzymes.

Human UGT enzymes are expressed in a tissue-specific manner. Most UGTs, including UGT1A1, UGT1A3, UGT1A4, UGT1A6, UGT1A9, UGT2B4, UGT2B10 and UGT2B7, are predominantly expressed in the liver [3,4] and expressed to a lesser extent in extra-hepatic tissues. Several UGTs are preferentially expressed in extra-hepatic tissues, including the kidney, small intestine, colon, stomach, lungs, epithelium, ovaries, testis, mammary glands and prostate. In particular, UGT1A7, UGT1A8, and UGT1A10 are highly expressed in the gastrointestinal tract, excluding the liver. This expression limits the bioavailability of orally administered drugs, such as raloxifene, naloxon, and mycophenolic acid, as well as xenobiotics, such as resveratrol and quercetin [5,6]. The intestine-specific expression of UGT1A8 and UGT1A10 was explained by transcriptional regulation through an intestine-specific transcription factor, caudal type homeobox 2 (Cdx2), as well as Sp1 and hepatocyte nuclear factor (HNF) 1α [7–10]. However, why UGT1A8 and UGT1A10 are not expressed in the liver, where Sp1 and HNF1α are abundantly expressed, remains unsolved.

The purpose of this study was to clarify the underlying mechanisms of the defective expression of UGT1A10 in the liver, focusing on epigenetic regulation. Although UGT1A8 mRNA is substantially detected in intestine, the expression of UGT1A8 protein has never been proven. In contrast, UGT1A10 protein could be clearly detected in the intestine by Western blot analysis using

* Corresponding author. Tel.: +81 76 234 4407; fax: +81 76 234 4407.
E-mail address: nmiki@p.kanazawa-u.ac.jp (M. Nakajima).
[1] Present address: Department of Drug Safety Sciences, Nagoya University Graduate School of Medicine, Nagoya, Japan.

0006-2952/$ – see front matter © 2013 Elsevier Inc. All rights reserved.
http://dx.doi.org/10.1016/j.bcp.2013.11.001